UiT

**THE ARCTIC
UNIVERSITY
OF NORWAY**

Faculty of Health Sciences, Department of Medical Biology
Tumor Biology Research Group

Regulation of urokinase receptor (uPAR) cleavage by cancer associated fibroblasts (CAFs) in oral cancer

—

Manyahilishal Etana Kitaw

Master's thesis in Biomedicine-June 2019

Table of contents

1. Acknowledgements

First, I praise God for His mercy and unconditional love that take care of me day and night and guide my life towards wisdom.

A special gratitude and admiration goes to my inspiring supervisor, Synnøve Magnusson, for giving me the opportunity to work with her, for her tireless efforts, guidance, critical comments, patience and unlimited encouragement throughout this thesis work. Once again, this would have not been possible without your all rounded support, thank you so much☺. My appreciations are also extended to my co-supervisors Professor Jan-Olof Winberg and Beate Hegge for their invaluable advice, guidance and support during my lab work and preparation of this thesis.

My appreciation also reaches out to Eli berg, Beante Mortensis, Rajita Dawadi and Susannah Von Hofsten for sharing their expertise during those difficult times of lab work. Thank you also for the smiles we shared in the lab☺.

The tumor biology research group, all of you, are so helping and inspiring. My special thanks to each of you for celebrating my special birthday with your lovely birthday song and gift. I always remember you.

My thanks also extend to my classmates for sharing me smiles even in those hardest times that energized me to keep going the path unstopping.

My respect and love always goes to my family for their love and encouragements to continue my education. My daughters, Ruth and Amen, you are my special gifts and sources of happiness all the time. My deepest respect and love goes to my husband, Shiferaw Jenberie, for supporting me in climbing up each step on the life's ladder. Lastly but not least, my dearest respect and love goes to my mom, Aselefech W., for her never ending support and pray to me and my family.

2. Abbreviations

CAF	Cancer associated fibroblast
CM	Conditioned medium
DMEM	Dulbecco's Modified Eagle's medium
DMSO	Dimethyl sulfoxide
DTT	Dithiothreitol
ECM	Extracellular matrix
HRP	Horseradish Peroxidase
MMPs	Matrix metalloproteinases
OSCC	Oral squamous cell carcinoma
PA	Plasminogen activation
PAI-1	Plasminogen activator inhibitor-1
PDGF	Platelet derived growth factor
PDGFR	Platelet derived growth factor receptor
RPMI	Roswell Park Memorial Institute
SFM	Serum free medium
TEMED	Tetramethylethylenediamine
TGF-β1	Transforming growth factor beta 1
TME	Tumor microenvironment
uPA	Urokinase plasminogen activator
uPAR	Urokinase plasminogen activator receptor
α-SMA	Alpha-smooth muscle actin
RIPA	Radioimmunoprecipitation assay

3. Abstract

Oral squamous cell carcinoma (OSCC) is one of the frequently diagnosed type of oral cancers and is a leading cause of cancer associated mortality and morbidity worldwide. Cancer associated fibroblasts (CAFs) are activated fibroblasts that are found in association with cancer cells. CAFs are the most abundant stromal cells in the tumor microenvironment (TME). In the TME, cell interactions mediated by different soluble factors released from both stromal cells and cancer cells play a crucial role in tumor progression and metastasis. Of these interactions, high expression of the serine protease urokinase (uPA) and its receptor (uPAR) and the uPA inhibitor (PAI-1) have all been associated in triggering invasion and metastasis. The aim of this project was to study CAFs role in regulation of uPAR cleavage. We also aimed to identify soluble factors involved in cleavage regulation. Artificial CAFs were made *in vitro* by activating 3T3 cells (fibroblasts) using transforming growth factor β1 (TGF-β1) and conditioned media (CM) from AT84 cells (CM-uPAR and CM-EV). CMs from activated fibroblasts were harvested and used to treat OSCC cells overexpressing uPAR. For this, we optimized a culture medium that enabled us to activate fibroblasts in a controlled manner by supplementing the basal medium (RPMI) with low FBS (0.5%) and ITS (1%). Flp-In 3T3 cells treated with TGF-β1 showed high expression α-SMA and had elongated shape, which is a characteristic morphology of activated fibroblasts. However, Flp-In 3T3 cells treated with CM-uPAR and CM-EV from AT84 cells did not show activated phenotype. AT84-uPAR cells treated with CM prepared from TGF-β1 treated Flp-In 3T3 cells (CM-Flp$^+$) revealed significantly (p=0.0005) higher full-length uPAR compared with CM-Flp$^{\div}$ treated cells. Gel-zymography analysis of CM-Flp$^+$ also exhibited the presence of high PAI-1 and matrix metalloproteinase 2 (MMP2). Thus, the detection of full-length uPAR might be due to the high PAI-1 expression that has a function of scavenging and inhibiting uPA activity as evidenced by low level of uPA in the CM-Flp$^+$. Immunohistochemistry was also used to study the relative CAFs infiltration in different uPAR expressing mouse tongue tumor sections. The immunoratio analysis revealed high CAFs infiltration in high uPAR expressing tongue tumor sections. Together, these findings suggest the regulatory interplay between CAFs and uPAR expression in OSCC. These findings, however, warrant further investigation using more functional assays that illustrate this interplay between CAFs and uPAR.

4. Introduction

4.1 Oral squamous cell carcinoma

Oral cancer is a type of head and neck cancer where any cancerous growth is located in oral cavity (1). More than 90% of the oral cancers are oral squamous cell carcinoma (OSCC) that arise from squamous or epithelial cells lining the oral cavity. OSCC is characterized by local invasion, a tendency for early metastasis to regional lymph nodes and has a high tendency to reoccur (2, 3). OSCC tends to occur in mobile part of tongue, floor of mouth, gingiva, cheek lining and roof of mouth (hard plate) (4). The tongue is the most frequently diagnosed site for the occurrence of OSCC (5, 6), which is rich in blood and lymphatic vessels on both dorsal and ventral parts that may favor metastasis (6).

4.1.1 Epidemiology of OSCC

OSCC is a common cause of morbidity and mortality (7-9). The global cancer statistics registered a higher incidence and death rate in male than female (10). The occurrence of cancer depends on the exposure to different risk factors. (1). Tobacco smokers are six-fold higher at risk of developing oral cancer than nonsmokers, and combination of tobacco and alcohol use increases the risk of oral cancer to fifteen fold (11). Chewing betel and paan, which is a mixture of betel and areca nut, is a known risk factor for the occurrence of oral cancer in many Asian countries (12). Other causes of oral cancer include poor oral hygiene, poor nutrition and chronic infections caused by fungi, bacteria or viruses (13).

4.1.2 Clinical features of OSCC

Early stages of OSCC development are usually painless; making the diagnosis of early stage OSCC a challenge to health practitioners. Later stages, however, are more painful and burning. The common clinical presentations include leukoplakia (whitish lesion), ulcer, pain, bleeding and difficulty with chewing, swallowing and speaking as well as weight loss. Most of the patients usually clinically presented with one or more lymph nodes involvement (8).

4.1.3 Treatment of OSSC

Treatment of choice depends on the localization and the extent of the primary tumor, the patient health status and desire. Oral cancer patients can be grouped based on TNM staging system and degree of differentiation, which are used to decide on the outcome as well as treatment of the patients. (14). OSCC are also further graded in to well or moderate (15). TNM classifies tumors according to the size and extent of the primary tumor (T1-4), absence or presence and extent of regional lymph node involvement (N0-3), the absence and presence of distant metastasis (M0-1). The standard treatment of oral cancer is surgery, which might be extensive, and/ or radiotherapy (16). For most advanced cases, radiotherapy prior to surgery is often the treatment of choice. Prognosis of OSCC depends on tumor size, efficacy of the treatment and patient immunity (17). Despite advances in the treatment of oral cancer, the mortality rate is still unchanged over the years and is around 50% (16). Genetically altered epithelial cells nearby the primary tumor are believed to be the important factor for reoccurrence after therapy (18). Of those who survived, around 4% become susceptible to the development of new independent secondary tumor (19). The overall 5-year survival rate is around 50% with combinatorial treatment of surgery and radiation (5).

4.2. Tumor microenvironment (TME)

The TME is an environment created by the tumor and dominated by tumor-induced interactions (Fig. 1) (20). The TME includes blood vessels, immune cells, fibroblasts, epithelial cells, growth factors and extracellular matrix (ECM) (21). TME is a complex environment where various interactive signaling taking place via different signaling molecules released by both tumor and stromal cells. Some components of TME, are summarized below.
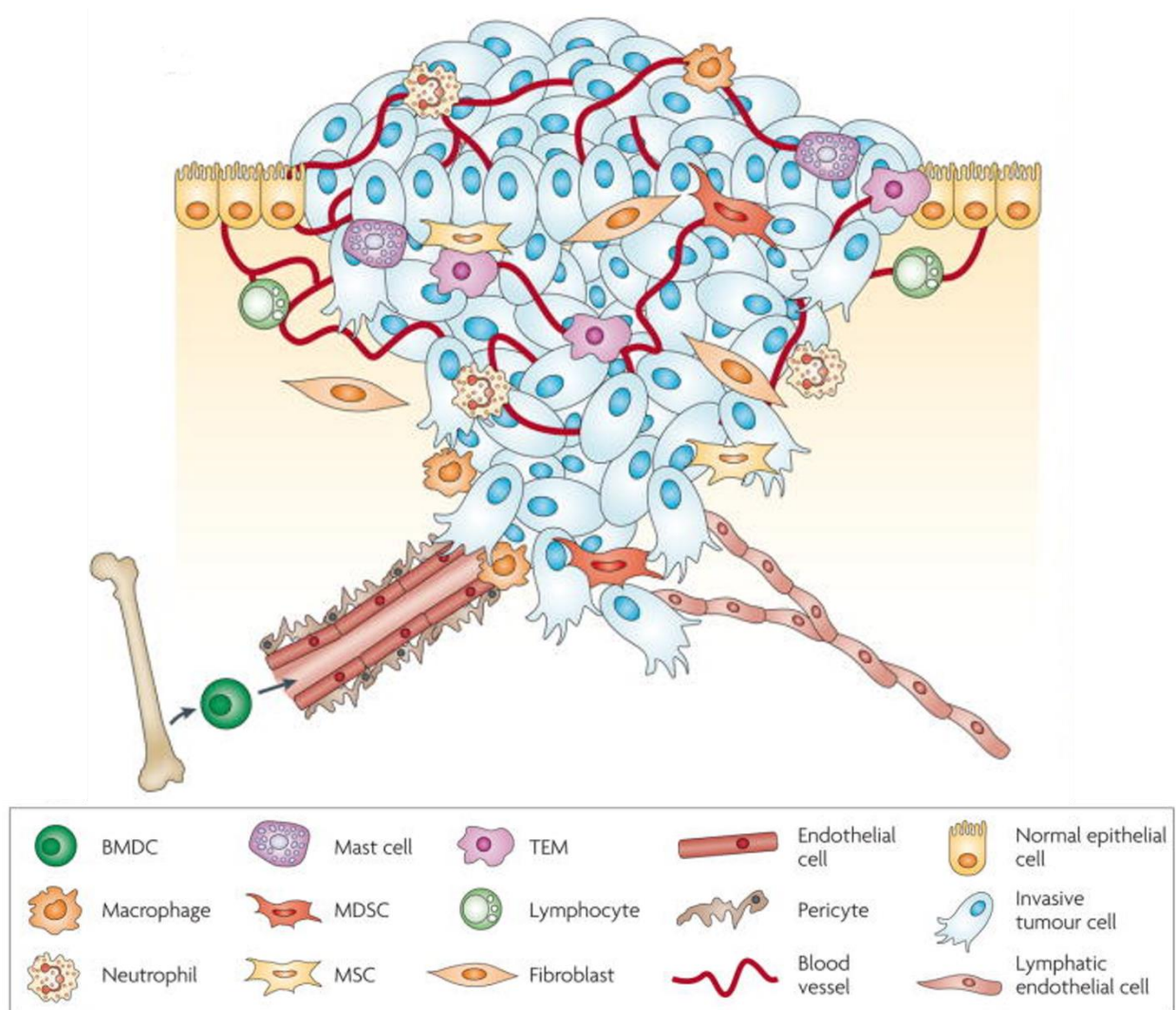
Figure 1. The Tumor microenvironment. *The tumor microenvironment contains numerous stromal cells that have either tumor suppressing or promoting function. This includes fibroblasts, endothelial cells, macrophages etc. Bone marrow derived cells (BMDC); myeloid dendritic stromal cells (MDSC); mesenchymal stromal cells (MSC); TIE2- expressing monocytes (TEM). Figure from (22).*

4.2.1. Extracellular matrix (ECM)

Extracellular matrix (ECM) has two forms; interstitial matrix and basement membrane. ECM has different components such as collagens, fibronectin, elastin, fibrillin, glycosaminoglycans and glycoproteins that give both structural and biochemical support to the surrounding cells (23). The interstitial matrix is the matrix found between cells (or interstitial space), which is filled by gels of polysaccharides and fibrous proteins (collagens) (24). Basement membrane is a fibrous matrix mainly composed of glycoproteins, type IV collagen and laminin, found between cellular element

and connective tissue. In cancer, the normal ECM structure is transformed by the reactive molecules such as MMPs and proteolytic enzymes secreted from stromal cells. The TME recruited stromal cells include vascular endothelial cells, pericytes, adipocytes, fibroblasts, and bone-marrow derived cells (25). The bulk of collagen I and III, fibronectin, proteoglycans and glycosaminoglycan that gives ECM the characteristics desmoplastic stromal appearance is mainly produced by CAFs (26). This increased amount of ECM secretion transform the initial fibrillar ECM into a dense acellular collagenous ECM, which is the hallmark of tumor associated stroma (26).

4.2.2. Cells in TME

4.2.2.1. Angiogenic vascular cells

Angiogenesis is the growth of blood vessels from the existing blood vessels through spurting and splitting. Angiogenesis is a multi-step process that involves tube forming endothelial cells and supporting perivascular cells pericytes and smooth muscle cells (27). Vascular endothelial growth factor (VEGF) plays a major role in regulating angiogenesis (28). VEGF with its receptor (VEGR) induce endothelial cell proliferation and development of angiogenesis (28). Thus, tumor associated blood vessels promote tumor growth by providing oxygen and nutrients and facilitate tumor cell entry to circulation to favor metastasis (29).

4.2.2.2. Immune cells

Diverse leukocyte subsets of both myeloid and lymphoid lineage cells infiltrate TME (30, 31). These immune cells include tumor-associated macrophages (TAM), immature myeloid cells that can possess suppressive activity, Tie2-expressing monocytes (32, 33), regulatory T cells (Treg), neutrophil and mast cells (34). The appearance of natural killer T cells and natural killer cells in TME predicts good prognosis (35). Tumor associated macrophages, programmed by Th2-type cytokines (IL-4, IL-5 IL-10 and IL-13) are abundant in most cancers and are usually tumorigenic (36).

4.2.2.3. Cancer associated fibroblasts (CAFs)

Activated fibroblasts, also called myofibroblasts or cancer associated fibroblasts, are the major stromal cells found in TME. Activated fibroblasts have more euchromatin, high rough endoplasmic reticulum, more Golgi apparatus and one or two nucleoli than normal fibroblast that has small nucleus, more heterochromatin and less rough endoplasmic reticulum (37). In normal condition, fibroblasts are mainly found embedded in loose fibrillar collagen I and fibronectin. Fibroblasts interact with their environment using integrin α1β1 cell surface receptor, which is connected to cytoskeletal actin and intermediate vimentin filament. Activated fibroblasts on the other hand secrete more ECM molecules comprised of collagen I, tenascin C, fibronectin containing the extra domain A (EDA-fibronectin) and secreted protein acidic and rich in cysteine (SPARC) (38-41). CAFs are derived from normal fibroblasts, pericytes, endothelial cells, circulating fibrocytes and bone marrow derived mesenchymal cells (42).

Task accomplished activated fibroblasts are removed via apoptosis (43). However, CAFs remain active in the reactive stroma, which is a new stromal environment in response to carcinoma, and become a prominent contributor in cancer (44, 45). CAFs are found in almost all forms of solid tumors and play an important role in cancer progression that include induction of epithelial-mesenchymal transition (EMT) and metastasis. EMT is the process by which epithelial cells lose the cell-to-cell adhesion and gain invasive and migratory property. CAFs play an important role in cancer progression by producing different growth factors (e.g. TGF-β) and cytokines (e.g. IL-4, IL-6) (46, 47) and inducing tumor proliferation in paracrine manner (48).

4.2.3. Growth factors

Growth factors secreted by cancer cells, endothelial cells and CAFs may regulate growth and proliferation (49). These include hepatocyte growth factor (HGF), insulin- like growth factor (IGF), epidermal growth factor (EGF), nerve growth factor (NGF), wingless/integrated protein 1 (WNT1), TGF-β and fibroblast growth factor 2 (FGF2) (50).

Platelet derived growth factor (PDGF) is secreted by many different types of cancer cells. PDGF has a chemotactic function and mitogenic activity on cells bearing its receptor, PDGFR. Both CAFs and macrophages are known to express PDGFR (26). Thus, PDGF is the most important growth factor in recruiting stromal cells and inducing their proliferation. Proliferation of stromal cells may impact the progression of cancer (51, 52). Recruited CAFs replace initial fibrin by collagen matrix. Therefore, its high expression has been related to tumor progression as explained by stromalization of tumors (26).

TGF-β is secreted mainly by platelets, but also produced by regulatory T cells, monocytes, macrophages, lymphocytes, fibroblasts, epithelial cells and dendritic cells (53-55). TGF-β is inactive when produced, which is complexed with latent TGF-β binding protein (LTBP) and latency associated protein (LAP) (56). The activation of TGF-β is induced during ECM degradation by different proteolytic enzymes (57, 58). Active TGF-β is also released by macrophages that endocytosed IgG bound latent TGF-β released by plasma cells. Other factors that including proteases, integrins (αVβ6 and αVβ3), pH and reactive oxygen species (ROS) have been described to induce the activation of latent TGF-β complex (59-61). The activated TGF-β binds to constitutively active TGF-β type II receptor, which then activate TGF-β type I receptor and induce phosphorylation. TGF-β functions as tumor suppressor during early stages of tumor development. However, at later stage it promotes tumor progression (62). Two known TGF-β signaling are SMAD pathway (canonical) and apoptosis via death associated protein 6 (DAXX) pathway in normal condition, while non-canonical pathway instead function with JNK-1, JNK-2 and p38 mediated signaling as reported in some degenerative diseases and cancer. The downstream signaling associated to non-canonical pathway (Fig. 2) include MAP kinase, Rho-like GTPase and phosphatidylinositol-3-kinase/AKT (63). The canonical pathway includes the phosphorylated TGF-β type I receptor then phosphorylates SMAD2 and SMAD3 proteins and then, the dimerized SMAD2/SMAD3 is translocated to the nucleus upon SMAD4 binding and it induces transcription of target genes (Fig. 2). In normal conditions, TGF-β inhibits growth via down regulation of c-MYC oncogene and inhibition of cyclin dependent kinases (CDKs) via

upregulation of p15INK4B and p21CIP1 and downregulation of CDC25A oncogene expression(64, 65).
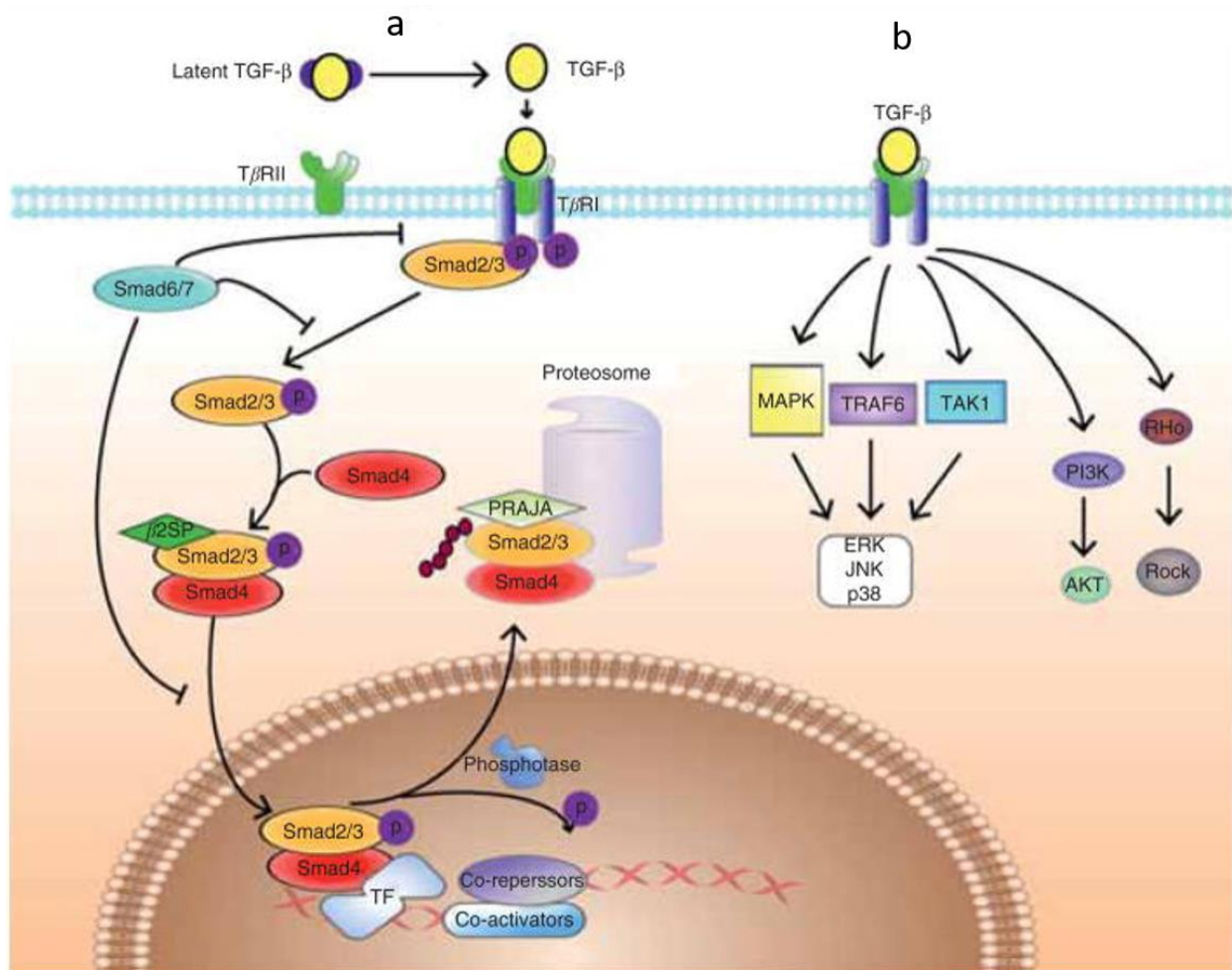
Fig 2. TGF-β signaling pathways. a. *SMAD dependent pathway where activated TGF-β binding induces phosphorylation of SMAD 2/3 and induce transcription of target genes.* **B.** *Non-SMAD dependent pathways where MAPK, PI3K and RHO signaling induced following ligand binding. Transcription factor-TF; tumor necrosis factor receptor associated factor 6 - TRAF6, mitogen activated protein kinase- MAPK; phosphoinositide 3' kinase – PI3K; extra cellular signal regulated kinases- ERK; c-Jun N-terminal kinase -JNK. Figure from (66).*

The non-canonical pathway has been reported to be activated by TGF-β that bound to its receptor and/ or mutation to the downstream signaling molecules other than SMADs (63) (Fig. 2). TGF-β activation induced ERK2 signaling in non-canonical pathway (67). ERK2 signaling results in EMT of normal epithelial cells during embryogenesis and cancer (68, 69). In addition, TGF- β mediated

PI3K/ AKT signaling has been reported to inhibit SMAD pathway and induce apoptosis, EMT and growth (Fig 3) (70-72).

4.2.4. Matrix metalloproteinases

Matrix metalloproteinases (MMPs) are zinc dependent endopeptidases (73, 74) that are expressed in small amount in normal physiological conditions when compared to pathological conditions. MMPs activity is controlled at three stages: at transcription, zymogen activation and inhibition of the active form by tissue inhibitor of metalloproteinases (TIMP) (75). MMPs are synthesized as inactive zymogen (pro enzymes) and are activated extracellularly. Dysregulation of the balance between MMPs and their inhibitors result in progression of certain degenerative diseases and cancer (76). The most known substrate-based MMPs groups include gelatinases (MMP2, MMP9), collagenases (MMP1, MMP8, MMP13) and stromelysins (MMP3, MMP110, MMP11). MMP2 and MMP9, function in cancer has been summarized as these were studied in this thesis.

4.2.4.1. Matrix metalloproteinase 2

Matrix metalloproteinase 2 (MMP2), also called collagenase IV or gelatinase A, which is 72KDa protein that has ECM proteolysis function. MMP2 is secreted by a variety of cells including endothelial cells, fibroblasts and activated fibroblasts during angiogenesis, wound healing, fibrosis and tumor invasion (77-79). MMP2 is secreted as an inactive proenzyme and activated by other proteases. MMP2 degrades collagen IV, a major component of the basement membrane, and result in loss of tissue organization that favors metastasis (80). Together with other MMPs, MMP2 also activates growth factors (e.g. TGF-β) to promote EMT and metastasis (77).

4.2.4.2. Matrix metalloproteinase 9

Matrix metalloproteinase 9 (MMP9), also called gelatinase B or collagenase type IV, is 92KDa protein. MMP9 is secreted by a wide number of cells such as macrophages, fibroblasts, neutrophils and endothelial cells (41). It is secreted as inactive proenzyme and activated by other

proteases (41, 81). MMP9 degrades ECM in both physiological (e.g. embryogenesis) and disease conditions (degenerative conditions and cancer) (41). In addition to collagen IV and V degradation (81), MMP9 has been involved in neutrophil migration (82), IL-8 dependent hematopoietic progenitor cells mobilization and endothelial cells migration during angiogenesis (83) (84). Most metastatic cancers have high expression of MMP9 (85, 86).

4.3. Plasminogen activation system

Plasminogen activation (PA) system is an enzymatic system involved in ECM degradation and turnover that promotes cancer invasion and progression (87). PA system comprises the serine proteases, urokinase plasminogen activator (uPA) and tissue plasminogen activator (tPA), their inhibitors, plasminogen activator inhibitor 1 (PAI-1) and plasminogen activator inhibitor 2 (PAI-2), and the cell surface bound uPA receptor (uPAR) (88, 89). Both tPA and uPA are found in TME; however, it is only uPA that has active role in tumor progression (90). PA system plays a major role in cancer progression via favoring invasion, migration, and metastasis (88). Higher expression of PA system components has been found in cancer than normal condition (91).

4.3.1 Urokinase plasminogen activator (uPA)

uPA, also called urokinase, is a serine proteinase of 55 kDa as pro-uPA, which is produced in all mammalian cells and is activated when binds to its receptor (89, 92). uPA is composed of two peptide chains bridged together by di-sulfide bond; amino terminal fragment (ATF) and carboxy terminal B-chain. The amino terminal contains the EGF-like and kringle domain. The EGF-like domain is the binding domain of the pro uPA or the active uPA while the kringle domain interacts with cell surface receptor. The carboxy terminal B-chain contains the catalytic serine protease domain (93-95).

uPA activates the conversion of the zymogen plasminogen to plasmin (96). Activated plasmin induces cleavage of pro-uPA into high molecular weight uPA (HMW-uPA). HMW-uPA is further cleaved into low molecular weight uPA (LMW-uPA) and ATF. The LMW-uPA has proteolytic function but is incapable of binding to uPAR (97, 98). uPA is irreversibly inhibited by PAI-1 and

PAI-2 (99), while α1-antiplasmin and α2-macroglobulin are inhibitors of plasmin (100). Serpine 1 (Nueroserpine 2), serpine 2 (PN), protein C inhibitor (PAI3), thrombin, and leukocyte elastase have also been reported as uPA inhibitors. High expression of uPA in cancer functions by degrading ECM via activation of plasmin, which in turn promotes cancer progression by facilitating tumor cell migration, proliferation and metastasis (101, 102).

4.3.2. Plasmin

Plasmin is a serine protease released as a zymogen called plasminogen from the liver into the systemic circulation. The activation of plasminogen takes place when it binds to fibrin clot or cell surface plasminogen-binding proteins. This activation induces a conformational change that allows enzymes such as such as tPA, uPA, trypsin, Kallikreins or coagulation factor XII bind to it and activate its conversion to plasmin. The cell surface plasminogen receptors include annexin II–S100A10, cytokeratin 8, α-enolase, plasminogen receptor (KT) (Plg-R(KT)) and histone H2B (103). The activation of plasminogen by uPA requires the presence of a co-factor, uPAR, on the cell membrane. Plasmin is involved in the degradation of the extracellular matrix (ECM) by activating matrix metalloproteinases (MMPs). Thus, plasmin is involved in tissue remodeling, tumor invasion and development of distant metastasis and angiogenesis (104, 105). High expression of plasmin, with its activators and inhibitors are reported in metastatic conditions (106)

4.3.3. Urokinase receptor (uPAR)

uPAR, also known as cluster of differentiation 87, CD87, is a glycosylphosphatidylinositol (GPI) anchored three domain (DIDIIDIII) receptor (107, 108) (Fig. 3). It is a high affinity uPA binding receptor, which lacks cytoplasmic domain (109). it interacts with other proteins extracellularly that include vitronectin, integrins, Low density lipoprotein receptor-related protein 1 (LPR-1), G-protein coupled receptor (GPCR) and Platelet derived growth factor receptor (PDGFR) (110-112). uPAR has many functions in cell signaling and it also interacts with different receptors (63). uPAR can be cleaved at both DI-DII linker and the GPI anchor region. Proteases like uPA, plasmin, MMPs and trypsin cleave uPAR at DI-DII linker region (113), while phospholipase C and D cleave uPAR

at the GPI anchor region (114-116). Therefore, fragments of uPAR are DI, DIIDIII, and soluble uPAR (suPAR also known as DI-III) (Fig. 3).
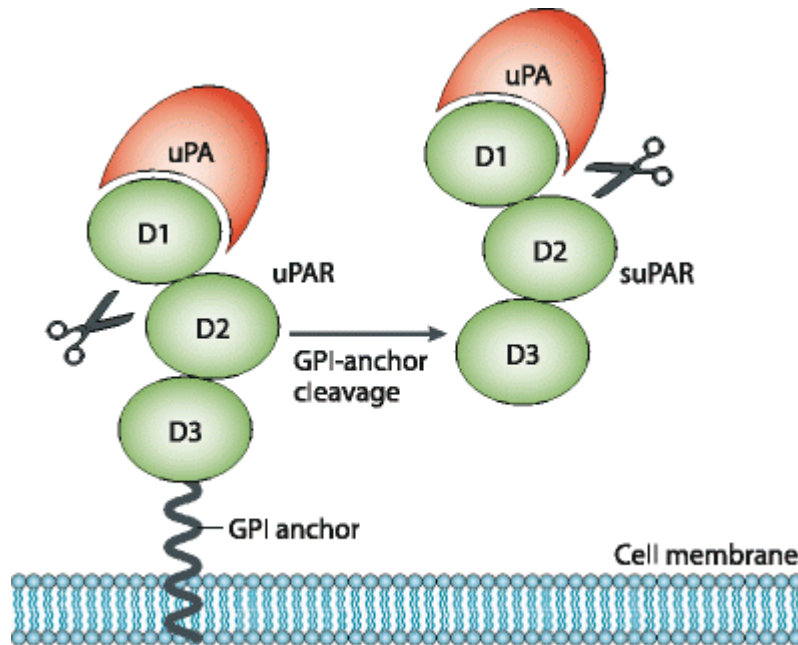
Figure 3. Schematic uPAR presentation. *uPAR is GPI anchored a three-domain receptor that bound to its ligand uPA. It shows GPI-anchor proteases cleavage and liberates a suPAR. Cell membrane bound uPAR and suPAR can also cleaved at DI-DII linker region by proteases and liberates DI and DIIDIII uPAR fragments. GPI- glycosylphosphatidylinositol, uPA- urokinase activator, uPAR- urokinase activator receptor, suPAR- soluble urokinase activator receptor. DI= D1, DII= D2 and DIII= D3. Image from (117)*

4.3.4. uPAR in cancer migration and metastasis

uPAR is highly expressed in stromal and cancer cells, and is involved in cancer invasion, migration and metastasis (108, 118). uPAR functions in both PA system dependent and independent manners. The PA system dependent function activates the proteolytic activity of proteases (109), while the PA system independent function with uPAR-vitronectin binding where it induce Rac signaling, that result in cell cytoskeletal rearrangement (110, 111, 119). In addition, uPAR re-expression at the leading edge of migrating cells suggests its role in migration (120). PA-dependent proteolysis activity could be inhibited through PAI-1 (108). uPAR with its co-receptors, integrins, signaling has been reported to promote tumor growth and metastasis (121).

4.3.5. The interaction of uPAR and fibroblasts

uPAR expression increases during fibroblast proliferation, while its expression is inhibited during myofibroblast differentiation and during fibrosis (112). Activated fibroblast secrets increased amount of proteases and growth factors. TGF-β promotes myofibroblasts phenotype, while FGF 2 promotes the normal fibroblasts phenotype. uPA inhibits myofibroblasts differentiation and favors normal fibroblasts phenotype (122). Expression of full length uPAR enhances cell adhesion and stabilize the cell attachments to ECM (123). The uPA-uPAR bound to the cytoskeletal attachment reported its importance in primary corneal fibroblasts migration (124).

4.4. OSCC markers

TME associated stromal cells and soluble factors markers are used in cancer studies. High VEGF and MMP11 expression in OSCC are associated with poor prognosis (125). Similarly, the combined high expression of p53, cyclin D1, and EGFR has been correlated with an adverse outcome in OSCC patient (126). In addition, high CD163 + macrophage (M2) infiltration in tumor stroma is associated with poor survival, while high CD57 + NK cells was significantly associated with improved overall survival (127).

The presence of CAFs is a strong predictor of poor prognosis of head and neck squamous cell carcinoma (128). Upregulation of podoplanin, a glycoprotein with mucin like function, in CAFs has been suggested a poor patient out come in oral cancer and breast cancer (129). Similarly, high expression of α-SMA in CAF has been correlated with tumor progression and poor prognosis (130). Recently, platelet derived growth factors receptor beta (PDGFRβ) was indicated as novel CAFs marker in OSCC (128). Other factors including fibroblast associated protein 1 (FAP-1), fibroblast specific protein-1 (FSP-1 also known asS100A4), metalloproteinases (MMPs) and secreted protein acidic and rich in cysteine (SPARC) have also been proposed as CAF specific markers (131).

5. The objectives of the study

Studies have shown that fibroblasts in TME are activated by different growth factors (e.g. TGF-β1) and cytokines (132). The activated fibroblasts (CAFs) in turn secretes increased amount of TGF-β, other growth factors and ECM proteins, that may enhance cancer cells migration and invasion (132). TGF-β1 regulate uPAR cleavage through the secretion of soluble factors (133). Moreover, the regulatory mechanism by which these soluble factors effect uPAR cleavage is started being investigated. Hence, we hypothesized that through the regulation of uPAR cleavage, CAFs regulate both proteolytic activity of cancer cells, and their ability to migrate and invade. This CAFs regulatory mechanism, therefore, could be a potential treatment target against cancer. We, therefore, set out the following objectives to contribute towards a better understanding of CAFs role in uPAR cleavage:

- Optimize conditions to activate fibroblasts with TGF-β and harvest conditioned media.
- Study the regulation of uPAR cleavage by using conditioned media harvested from activated and non-activated fibroblasts.
- Identify soluble factor (s) released from activated or non-activated fibroblasts that regulates uPAR cleavage

6. Materials and Methods

6.1. Materials and instruments

Materials and instruments used	Producer
10x Glycobuffer 2 (lot # 0041709)	BioLabs Inc., New England
12 well and 96 well plates (REF # 353072)	FALCON, Life Sciences, USA
Acrylamide	BDH Chemical Ltd., Poole, UK
BioDoc-It®220 Imaging Systems (S/N B111110-010)	UVP imaging, California, USA
Bioruptor® PLUS (Cat # UCD-300)	Diagenode Inc., USA
Biotinylated ladder (lot # 7727)	Cell Signaling Technology, Norway
Bovine serum albumin (BSA- 2 mg/ml; lot # 23209)	Pierce, USA
Cell invasion and migration plate (CIM plate, 16, lot # 20171126)	ACEA Biosciences, Inc., San Diego, USA
Cells scraper, micro-pipetter and micro-pipette tips	Thermo scientific, Mexico
CellTiter 96 Aqueous One Solution Cell Proliferation Assay (Cat # G3582, lot # 0000311968)	Promega (Madison, WI 53711-5399 USA)
Chemiluminescence peroxidase substrate-3 (CPS-3, C7364)	Sigma, USA
Countess II automated cell count (Cat # AMQAX1000)	Invitrogen, USA
DC Protein Assay kit (SIG 093094)	Bio-Rad Laboratories, USA
Diaminobenzidine (DAB) substrate and DAB chromogen	DAKO, California, USA
DPX Mountant (lot # BCBG9433V)	Sigma, USA
Dulbecco's Modified Eagle's medium (DMEM, D5796, Lot # RNBG7136)	Sigma, USA
Fetal bovine serum (S181BH, 5158705181B)	Invitrogen, USA
Gelatin	Sigma, USA
Glycoprotein denaturing buffer (lot # 10017111)	BioLabs Inc., New England
Goat serum (X0907, lot # 20031843)	DAKO, California, USA
Human platelet derived TGF-B (lot # AV7118061)	RD system,Bio-techne, UK
Immobilon-P PVDF transfer membrane (Cat # IPVH00010),	Merck Millipore, USA
Insulin transferrin selenite (ITS, Cat # I1884)	Sigma, USA
LAV-3000 Imaging system	Fujifilm, Tokyo, Japan

MES SDS running buffer (20x),	Invitrogen, UK
Micro-pipetter and micro-pipette tips	Thermo scientific, Mexico
M-pore Direct detect instrument	Merck Millipore, USA
NUPAGE 4-12% bis-Tris SDS-gels (REF # 18060671-2643, 12 well; REF # NP0322BOX, 10 well gel)	Invitrogen, UK
Phosphate buffer saline (PBS, 0914E)	Merck Millipore, Germany
Pipette tips (10 ml, REF # 356551; 5 ml, REF # 356543),	FALCON, Life Sciences, USA
Plasminogen (lot # 3104258)	Merck Millipore, USA
PNGase F kit (P07045) comprising of 10% NP-40 (lot # 0161801), PNGase F (lot# 10008073)	BioLabs Inc., New England
Protease inhibitor (lot # SLBV1198)	Sigma, USA
Re-Blot Plus mild Solution (lot # 3075152)	Merck Millipore, USA
Recombinant mouse soluble uPAR HIS-(CSI 20008A)	Cell Science, USA
Roswell Park Memorial Institute (RPMI)-1640 medium (R8758, Lot # RNBG8807),	Sigma, USA
SeeBlue prestained (lot # 929080)	Invitrogen, USA
T25 and T75 cell culture flasks	FALCON, Life Sciences, USA
Titramax 101 Plate shaker (S/N. 010609811)	Heidolph, Germany
Triton X-100 (lot # STBH6272)	Sigma, USA
Trypsin-EDTA solution (0.25%, SLBS7958)	Sigma, USA
VERSAmaxPLUS microplate reader	Molecular devices, California, USA
Vortex mixer (lot # 110627098)	VWR international, Germany
Western blotting luminol reagents (sc- 2048)	Santa Cruz Biotechnology, USA
xCelligence Real time cell analysis - dual plate (RTCA DP) instrument	ACEA Biosciences, Inc., San Diego, USA
XCell SureLock electrophoresis System	Invitrogen, UK

6.2. Antibodies

Antibodies	Producer
Anti-Bactin-peroxidase antibody produced in mouse (lot. # 043M4825V, Monoclonal 1:1000)	Sigma, USA
Anti-α-Tubulin antibody (ab4074, Polyclonal, Rabbit, 1µg/ml)	Abcam, USA
Goat-anti-mouse uPAR antibody (AF534, polyclonal, 1:1000 dilution)	RD system, Minneapolis, USA
Goat-anti-rabbit HRP-linked (Cat # 4050-05, lot # 15114-T3651, 1:1000)	Southern Biotech, Birmingham, UK
HRP linked anti-biotin (7075P5, lot # 34)	Cell Signaling Technology, Norway
HRP linked anti-goat/sheep (A9452, 1:160,000)	Sigma, USA
Polymer-HRP anti-Rabbit peroxidase (K-4011, lot. 10109948, two drops per section)	DAKO, California, USA
Rabbit-anti- mouse α-SMA antibody (Ab5694,1:1000)	Abcam, USA
Rabbit-anti-mouse PAI-1 antibody (Ab28207, 1:2500)	Abcam, USA
Recombinant goat- anti-mouse uPAR primary antibody (AF534, 1:1000)	RD system, Bio-techne, UK

6.3. Cells

Name of cells	Source
AT84-uPAR cells and AT84-EV cells	AT84 cells were kindly provided by professor Shillitoe (134). The cells were transfected with uPAR and EV + shRNA by Synnøve (38)
Flp-In 3T3 cells (R761-07)	Invitrogen, Life technologies, California, USA and kindly provided by Ingvild Mikkola (39)

6.4. Tissue sections

Tissue section	Source
Tongue tumor sections	Provided by Synnøve Magnussen (38)
Xenografts and carcinogen induced tongue tumor sections	Provided by Elin Hadler-Olsen (135)

6.5. Software

Software	Source
GraphPad Prism version 5	GraphPad Software Inc., CA, USA
ImageJ	National Institutes of Health and the Laboratory for Optical and Computational Instrumentation (LOCI), University of Wisconsin
Immunoratio (153.1.200.58:8080) website	Institute of Biomedical Technology, University of Tampere

6.6. Composition of buffers and solutions

6.6.1. Buffers and solutions used in western blot

<u>NuPAGE running buffer- 600 ml</u>

NuPAGE MES SDS Running Buffer (20x)- 30 ml

Milli-Q water- 570 ml

<u>Blotting buffer- 1L</u>

Tris (base; MW: 121.14 g/mol)- 5.7 g

Glycine (MW: 75.067 g/mol)- 29 g

Methanol- 200 ml

Milli-Q water- 800 ml

TBST – 1X (Tris-buffered saline solution with Tween): 1L

5M NaCl- 30 ml

1M Tris pH 8.0- 20 ml

100% Tween 20- 20 ml

Milli-Q water- 950 ml

Blocking buffer- 5% milk

Non-fat dry milk powder- 4 g

1x TBST- 80 ml

Loading buffers:

5x sample buffer- 25 ml

0.25M Tris-HCl pH 6.8- 6.25 ml

Sucrose= 5 g

20% SDS- 12.5 ml

Bromophenol blue- 0.05 g

Milli-Q water- 7 ml

1x sample buffer:

5x sample buffer- 200 µl

Milli-Q water- 800 µl

Molecular weight marker:

Biotinylated protein ladder- 10 µl

SeeBlue®Prestained- 5 µl

Chemiluminescent peroxidase Substrate-3

Chemiluminescent reagent and Chemiluminescent buffer were mixed 1:1 ratio and kept at room temperature (RT) for 30 min prior to adding to probed membrane. Then can be re-used for a 2-3 times if kept cold.

6.4.2. Buffers and solutions used in SDS gel zymography

Separating gel buffer (1.5 Tris and 0.4% SDS with pH 8.8, 100 ml)

Tris (base; MW: 121.14 g/mol)- 18.2 g

SDS- 0.4 g (20 % SDS)- 2 ml

Milli-Q water added to give an approximate volume of 60 ml

pH was adjusted to 8.8 using 5M HCl

Milli-Q water added to give a total volume of 100 ml

Stacking/concentrating gel buffer (0.5M Tris and 0.4% SDS with pH 6.8)-10 ml

Tris (base; MW: 121.14 g/mol)- 0.605 g

SDS- 0.04 g

Milli- Q water added to give an approximate volume of 6 ml

pH was adjusted to 6.8 using 5M HCl

Milli Q water added to give a total volume of 10 ml

2 % Gelatin

gelatin bloom 300- 0.2 g

Milli-Q water- 10 ml

Separating gel for gelatin zymography (7.5% for one gel)

Separating gel buffer- 1120 µl

2% gelatin- 225 µl

Milli-Q water- 2266 µl

40% Acrylamide- 874 μl

Tetramethylethylenediamine (TEMED)- 7 μl

10% Ammonium persulfate- 15 μl (added just prior to pouring into gel cassette to avoid polymerization)

Separating gel for plasminogen zymography (7.5% for one gel)

Separating gel buffer- 1120 μl

2% gelatin- 225 μl

Plasminogen- 45 μl

Milli-Q water- 2221 μl

40% Acrylamide- 874 μl

Tetramethylethylenediamine (TEMED)- 7 μl

10% Ammonium persulfate- 15 μl (added just prior to pouring into gel cassette to avoid polymerization).

Stacking gel for zymography (4% for one gel)

Stacking gel buffer- 186 μl

Milli-Q water- 1145 μl

40% Acrylamide- 155 μl

TEMED- 4 μl

10% ammonium persulfate- 8 μl (added just prior to pouring into gel cassette to avoid polymerization)

Electrophoresis buffer, pH 8.3 (10x)- 1L

Tris (base; MW: 121.14 g/mol)- 30 g

Glycine (MW: 75.07 g/mol)- 144 g

SDS (final conc. 1.0%)- 10 g

pH adjusted to 8.3 with 5M HCl

Milli-Q water- 0.6 L-1 L

Washing buffer (2.5% Triton)- 400 ml

Triton X-100 (warm)-10 ml

Milli-Q water- 390 ml

Incubation buffer 10x (0.5 M Tris, 2M NaCl, 0.05M CaCl$_2$, 0.2% Brij- 35, pH 7.8)- 1 L

Tris (base; MW: 121.14 g/mol)- 12.1 g

Tris HCl (MW: 157.60 g/mol)- 63.0 g

NaCl (MW: 58.44 g/mol)- 117 g

CaCl$_2$.2H$_2$O (147.01 g/mol)- 7.4 g

30% Brij-35- 6.7 g

Milli-Q water added to a final volume of 1 L.

Incubation buffer 1x:

10x incubation buffer- 100 ml

Milli-Q water- 400 ml

Staining stock solution- 200 ml

Coomassie brilliant blue powder- 0.8 g

Methanol- 120 ml

Milli-Q water- 80 ml

Staining solution- 50 ml

Staining stock solution- 25 ml (first filtered)

20% acetic acid- 25 ml

De-staining solution- 400 ml

Methanol- 120 ml

100% acetic acid- 40 ml

Milli-Q water- 240 ml

Loading buffer

5x sample buffer

0.25M Tris-HCl pH 6.8- 6.25 ml

20% SDS- 12.5 ml

Sucrose- 5 g

Bromophenol Blue- 0.05 g

5x sample buffer was used for sample loading.

1x sample buffer (diluted with Milli-Q-water) was used for loading positive controls

Buffer used in cell culture and immunohistochemistry (IHC) methods

RIPA buffer-200 ml (Tris-HCl, pH 7.6- 2.5mM, Triton X-100- 1%, Sodium Chloride- 0.15 M, Sodium dodecyl sulfate (SDS)- 0.1%, Na-deoxycholate- 0.5%)

Tris-HCl, pH 7.6- 0.06 g

Triton X-100- 2 g

 Sodium Chloride- 0.03 ml

Sodium dodecyl sulfate (SDS)- 0.2 g

 Na-deoxycholate- 1g

Phosphate buffer saline- 1xPBS- 5 L

Phosphate buffer saline (9.55 g/L)- 47.75 g

Milli-Q-water- 5 L

Blocking buffer for IHC- 1.5% goat serum- 1 ml

100% goat serum- 15 µl

Milli-Q-water- 985 µl

6.5. Methods

6.5.1. Cell culture

6.5.1.2. AT84-uPAR cells and AT84-EV cells

The mouse oral squamous carcinoma cell line (OSCC), AT84 cells, used in this experiment were originally isolated from spontaneous oral cancer of C3H mouse cells (21). AT84 cells express low endogenous uPAR (38). As described elsewhere, the AT84 cells were made to stably express uPAR and shRNA targeting uPAR with empty vector, and are called AT84-uPAR and AT84-EV cells, respectively (38). Cells were taken out from liquid nitrogen, thawed, mixed with 15 ml of RPMI supplemented with 10% FBS and cultured at 37 ^{o}C, 5% CO_2 humid incubator. The cells were allowed to adhere for three hours before the medium was changed to remove the freezing medium, DMSO with 90% FBS. Cells were split at 80-90% confluence. Cells were routinely tested for mycoplasma contamination and were negative. All incubations of the AT84 cells were performed at 37 ^{o}C, 5% CO_2 humid incubator.

6.5.1.3. Flp-In 3T3 cells

Flp-In 3T3 cells are mouse embryonic fibroblasts cell lines, which were originally obtained from NIH Swiss mouse embryo by George Todaro and Howard Green in 1962 (40). Flp-In 3T3 cells contain a single stably integrated flippase recombination target (FRT) site by transfecting with pFRT/ lac Zeo vector. Flp-In 3T3 cells were taken out from liquid nitrogen and thawed. Cells were allowed to attach in T75 cell culture flasks containing 15 ml DMEM with 10% FBS and kept at 37 ^{o}C, 5% CO_2 humid incubator. Once attached the medium (DMEM with 10 % FBS) was changed and the same medium was also used for regularly culturing. All incubations with Flp-In 3T3 cells were performed at 37 ^{o}C, 5 % CO_2 humid incubator.

6.5.2. Medium optimization

Medium optimization was performed using CellTiter 96 Aqueous One Solution Cell Proliferation Assay to find a condition in which Flp-In 3T3 cells survived for 72 hours. In this assay, 7000 cells per well were seeded in three 96 well plates with either DMEM or RPMI containing 10% FBS and incubated overnight. Cells were then treated with DMEM or RPMI (100 µl) supplemented with

different concentrations of serum and ITS to determine the percent viability at 24, 48 and 72 hours. Media supplements used were ITS (1:100), 0.1% FBS, 0.1% FBS + ITS, 0.5% FBS, 0.5% FBS + ITS, 2% FBS, 2% FBS + ITS, and 10% FBS. Triton X-100 was used as a negative control, while 10% FBS supplement was used as positive control. Twenty µl of CellTiter 96 Aqueous one Solution reagent was added to each well and incubated further for two hours at 37°C, 5% CO_2 according to the company's protocol. During the two hours incubation, the CellTiter reagent was bio-reduced by metabolically active cells that changes the color of the medium to brown, while negative control wells (with no cells) remained unchanged, yellow. Then, the absorbance (optical density, OD) was measured at 490 nm using a 96-well plate reader. The OD values are directly correlated with percent survival. The percent survival was analyzed according to the company's instruction.

6.5.3. Activation of Flp-In 3T3 cells

Flp-In 3T3 cells were seeded in a 12-well plate at a concentration of $5x10^4$ per well. Cells were treated with RPMI containing human platelet-derived TGF-β1 (2 ng/ml), 0.5% FBS and ITS (1:100) for 72 hours. The media was changed every 24 hours to ensure continuous supply of TGF-β1. The medium was removed and washed 3x with 1xPBS and the cells were harvested using RIPA buffer. The cell lysates were sonicated. Then, the lysates were analyzed by western blot using anti-α-SMA antibody in a 2-µg total protein per lane to determine the activation status of Flp-In 3T3 cells.

6.5.4. Condition media preparation

6.5.4.1. Condition media preparation from activated and non-activated Flp-In 3T3 cells

Flp-In 3T3 cells, $1x10^6$ cells, were seeded in T75 flasks and treated with or without TGF-β1 (2 ng/ml) in 8 ml of supplemented RPMI (0.5% FBS and 1:100 ITS) for 72 hours. The medium was changed to RPMI (SFM) containing ITS (1:100) after 3x wash with 5 ml PBS to remove residual TGF-β1. After 24 hours of incubation, the conditioned media (designated here after CM-Flp⁺ for TGF-β1 treated and CM-Flp± for TGF-β1 untreated) (Table 1) were harvested, spun down to remove cells and kept in a freezer aliquoted in a 1 ml tube, ready for use.

6.5.4.2. AT84-uPAR and AT84-EV condition media preparation

Both AT84-uPAR and AT84-EV cells, 1×10^7, with RPMI plus ITS (1:100) were seeded in different T75 flasks, which were precoated with RPMI containing 10% FBS. The conditioned media (designated here after CM-uPAR for CM obtained from AT84-uPAR cells and CM-EV from AT84-EV cells) (Table 1) were harvested after 24 hours, spun down, dispensed in 1 ml tube and kept at -20 °C.

6.5.5. Activation of Flp-In 3T3 cells by CM-uPAR and CM-EV

Flp-In 3T3 cells, 5×10^4 per well, were seeded in 12 well plates. After overnight culture for attachment, they were treated with CM-uPAR and CM-EV mixed with RPMI containing 0.5% FBS and ITS (1:100) in 1:2 ratio (one portion fresh media with two portion of CM) for 72 hours. The control cells received RPMI containing 0.5% FBS and ITS (1:100). The medium was replenished daily except the third day, where serum was withheld from the medium. After 72 hours, the conditioned media (designated here after CM-Ctrl for CM harvested from control cells, CM-uPAR-Flp for CM-uPAR treated cells and CM-EV-Flp for CM treated with CM-EV) (Table 1) were harvested, spun and stored at -20°C. The CMs were analyzed for presence of changes in proteases concentration using gelatin and gelatin-plasminogen zymography, while the cells were harvested to analyse the activation of Flp-In 3T3 cells using western blot with α-SMA antibody and HRP linked goat-anti-rabbit antibody.

Table 1. Conditioned media (CM) prepared. The naming and description of the different conditioned media prepared and used the different assays.

CMs labeling	CM description	Use in this study
CM-Flp$^+$	CM harvested from Flp-In 3T3 cells treated with TGF-β1	To treat AT84-uPAR cells
CM-Flp$^÷$	CM harvested from Flp-In 3T3 cells not treated with TGF-β1 (control)	
CM-Flp$^+$-uPAR	CM harvested from AT84-uPAR cells treated with CM-Flp$^+$	

CM-Flp‡-uPAR	CM harvested from AT84-uPAR cells treated with CM-Flp‡	
CM-uPAR	CM harvested from AT84-uPAR cells	To treat Flp-In 3T3 cells
CM-EV	CM harvested from AT84-EV cells	
CM-uPAR-Flp	CM harvested from Flp-In cells treated with CM-uPAR	
CM-EV-Flp	CM harvested from Flp-In cells treated with CM-EV	
CM-Ctrl	CM harvested from Flp-In cells treated with RPMI + ITS.	

6.5.6. Treatment of AT84-uPAR cells with CM-Flp$^+$ and CM-Flp‡

AT84-uPAR cells, 2×10^5 per well, were seeded in 12-well plates in three parallels and cultured overnight with RPMI supplemented with 10% FBS. Cells were then washed 3x with PBS (1 ml) and treated with 1 ml of CM-Flp$^+$ or CM-Flp‡ overnight. After harvesting the conditioned media (designated here after CM-Flp$^+$-uPAR for CM harvested from CM-Flp$^+$ treated cells and CM-Flp‡-uPAR for CM-Flp‡ treated cells), the cells were lysed with RIPA buffer and harvested by scraping.

6.5.7. Analysis of uPAR expression and cleavage

The cell lysates from AT84-uPAR cells treated with CM-Flp$^+$ or CM-Flp‡ were analyzed for uPAR cleavage after sonication using Bioruptor® PLUS. A total protein concentration of 10 µg, measured using the direct detect method or the DC protein assay, were de-glycosylated as described below and analyzed for the expression of uPAR. The uPAR protein expression in the lysates (both cleaved- DIIDIII, and full length- DI-III) were determined using western blot with goat anti-mouse uPAR antibody and HRP linked anti-goat/sheep secondary antibody.

6.5.8. De-glycosylation

Protein de-glycosylation was performed using PNGase F kit according to the manufacturer's instruction. PNGase F is an enzymatic method used for removing almost all N-linked

oligosaccharides from glycoproteins (23). Cell lysates of 10 µg total protein was mixed with 1 µl 10x glycoprotein denaturing buffer and water (to adjust 10 µl final volume) and kept in boiling water for 10 minutes. Then, to make 20 µl reaction volume, 2 µl of 10x glycobuffer 2, 2 µl of 10% NP-40, 5.5 µl water and 0.5 µl PNGase F were added and incubated at 37°C for one hour. Samples were then analyzed using western blot.

6.5.9. Cell counting

In all the experiments, the cell count was performed on countess II automated cell counter using 0.4% trypan blue to differentially exclude the dead cells from viable. Cell suspension, 10 µl, was mixed with 10 µl of trypan blue, and 10 µl of the mix was filled into the counting chamber (slide). The slide was inserted into the countess II and both viable and dead cells were counted and the number of cells per ml was obtained. Based on the viable cell count, the required number of cells were calculated and seeded for the intended experiments.

6.5.10. Protein measurement

Cell lysates contain a different mixture of proteins. To determine the yield of specific proteins using western blotting, it is important to normalize the samples analyte into equal total protein concentration. Currently, different assays are available to quantify total proteins, which have different sensitivity and work under different conditions. In this experiment, direct detect protein quantification assay and DC protein quantification assay were used. Samples having less than 1.5 mg/ml total protein concentration were measured with DC protein Bio-Rad detection method, while samples over 1.5 mg/ml concentration were measured with Direct detect protein quantification method.

For Direct detect method, 2 µl sonicated cell lysates were pipetted into each circular areas/spots on a detection card and RIPA buffer (2 µl) was used as a blank. A program on the direct detect protein quantification device was opened and protein concentration was selected from INISTBSA AM2.93 program. Then, spots were labeled on the program according to the position of samples

(colored as green) and blank (blue colored) on the card following sample drying. Then the measurement of total protein (mg/ml) was determined for the respective loaded spots.

DC protein assay is a colorimetric assay following detergent solubilization in the reaction mix. In this assay, copper-treated proteins reduce folin reagent by losing 1, 2 or 3 oxygen atoms and result in a characteristic blue color development (136, 137). Different concentrations of BSA were used to plot a standard curve. The BSA concentrations used for standard curve were 0.2, 0.35, 0.5, 0.65, 0.75, 0.85, 1 and 1.5 mg/ml. A mixture of 25 µl reagent A (an alkaline copper tartrate solution) and reagent S (surfactant solution) (1:20) was added in each well containing sample or standard (5 µl). Subsequently, 200 µl of reagent B (a dilute folin reagent) was added to all wells and incubated at RT for 15 minutes on a shaker. Then, the OD value was measured at 750 nm with SoftMax pro software using 96 well plate reader. The total protein concentration for each sample was calculated according to the equation derived from the standards' concentrations. Sample protein concentration fell outside the concentration range covered by the standards was reanalyzed.

6.5.11. Western blot

Western blotting is a technique in molecular biology, which is used to detect a protein of interest in the mixture of proteins in the cell lysate or tissue homogenate. The proteins in the samples are separated by gel electrophoresis using sodium dodecyl sulphate buffer and poly acrylamide gel (SDS-PAGE). SDS-PAGE maintains the polypeptides in their denatured state once they are treated by reducing agents (SDS, DTT and heat) that remove the secondary and tertiary structures (di-sulfide bond, S-S to sulfhydryl, SH and SH). The proteins covered with negatively charged SDS migrate to a positively charged anode through the mesh of acrylamide gel according to their molecular weight when the voltage is applied along the gel. The speed of migration of proteins in the gel results in the separation of proteins. The concentration of acrylamide determines the resolution of proteins.

Western blot was performed to detect the expression of protein of interest in the samples. Samples were reduced and denatured with DDT (0.3M) and heat (100ºC for 10 minutes) before loading to NuPAGE 4-12% Gel. MES SDS running buffer was used for running the samples using XCell SureLock Electrophoresis System. PVDF membrane was activated in methanol (3 seconds) and rinsed successively in water (10 seconds) and blotting buffer (> 5 minutes) to ensure protein binding. The separated proteins on the gel were then transferred to PVDF membrane. The membrane was washed 1x with TBST (5 minutes) and incubated at RT with 5% blocking buffer for 40 minutes to block nonspecific binding. The blotted membrane was incubated with specific primary antibody overnight at 4ºC followed by 3x wash with 1xTBST for 5 minutes each and probed with secondary antibody for 1 hour at RT. Finally, to visualize the proteins of interest, the membrane was developed with western blotting luminol reagents and chemiluminescent peroxidase substrate-3. LAS3000 software was used for imaging. The expression level of the proteins of interest was analyzed using ImageJ software.

ImageJ analysis of band intensity was performed by taking equal sized rectangular area on each band of parallel lanes in a gray scale 8-bit image. Then the software generated parabolic curve, where the area measurement of each curve represented the expression. Each protein expression was normalized using relative intensity of its loading control. The peak loading control intensity was considered as a standard and loading controls for other samples were normalize by dividing to this peak value. The expression of the target protein was determined by multiplying to its normalized loading control as shown by the formula below.

- Peak loading control= standard= S
- Loading control for sample x= X
- Normalize loading control for sample x= X/S
- The expression of protein of interest y= Y
- The normalized expression of y= Y*(X/S)

6.5.12. Zymography

Zymography is an electrophoretic technique used to detect hydrolytic enzymes based on the substrate used in gel formation. Three different types of zymographys are available, namely in-gel, in-situ and in-vivo zymography (138). We used in-gel zymography, where gelatin and plasminogen were used as substrates to detect the presence of gelatinases (MMP2 and MMP9) and plasminogen activators (plasmin and uPA), respectively.

The separating gel (7.5% acrylamide) constituents were mixed as described in material section. Then, the gel mix was poured into a cassette and water was added to remove air bubbles, which can interfere with polymerization, and give a smooth shape. After 15 minutes of polymerization, the added water was removed and the stacking gel (4% acrylamide) was added. Then, a 15-tooth comb was inserted on the stacking gel before polymerization. After the gel was set, the cassette was dismounted and the gel was transferred to an electrophoresis chamber. Seventy milliliter 1x electrophoresis buffer was added on the upper part of the chamber, which supported the gel, and 70 ml was added in the lower part of the chamber. Then, the comb was taken out from the gel and standards, controls and samples were loaded. Electrophoresis was run for one hour and 30 minutes. The gel was then transferred to a petri-dish containing wash buffer (2.5% Triton X-100) and washed twice for 30 minutes on a shaker at RT to remove the SDS before incubated overnight at 37°C with the developing buffer. The gel was then stained with staining solution (Coomassie blue and 20% acetic acid mixture) for one hour at RT on a shaker. The gel was de-stained in de-staining buffer for 20-30 minutes followed by transfer to water bath for imaging. A clear band with a blue background shows the activity of proteolytic enzymes.

6.5.13. Real time cell analysis of migration

Real-time cell analysis using the xCELLigence was used to study cell migration. Flp-In 3T3 cells, 2000 cells per well, were seeded in cell invasion and migration plate 16 (CIM plate 16) in 100 μl of SFM with different concentration of chemoattractants, listed below. The CIM-plate 16 has two compartments, namely lower chamber and upper chamber, and a lid (Fig. 4a). The upper chamber is composed of porous membrane, where the cells enter through and has gold electrode

underneath where adhered cells detected. The lower chamber is used to hold the attractant medium. The lower chamber was filled up with 160 µl of CM in duplicates as shown below. Then, the upper chamber was assembled to the lower chamber and 50 µl SFM (DMEM) was added in each well, equilibrated at 37°C for one hour and background measurement was taken (Fig. 4b). Cells, 2000 cells in 100 µl of SFM (DMEM), were added to each upper chamber well except in wells that were used for no cells control or negative control. The setup was left at RT for 30 minutes for cells settlement. Then the CIM plate was mounted to the xCELLigence RTCA DP instrument (Fig. 4c) and the cell migration index measurements were performed in a work station (Fig. 4d). The cell index (CI), measure of the relative change in the electrical impedance, was registered every 15 minutes interval in the workstation system. Cell migration index at 12 hours was extracted from three independent experiments. Chemoattractants were loaded in duplicate, which included negative control, SFM (DMEM), DMEM supplemented with 10% FBS as a positive control, CM-uPAR, CM-EV and 10 ng/ml, 500 ng/ml and 10 µg/ml recombinant uPAR.
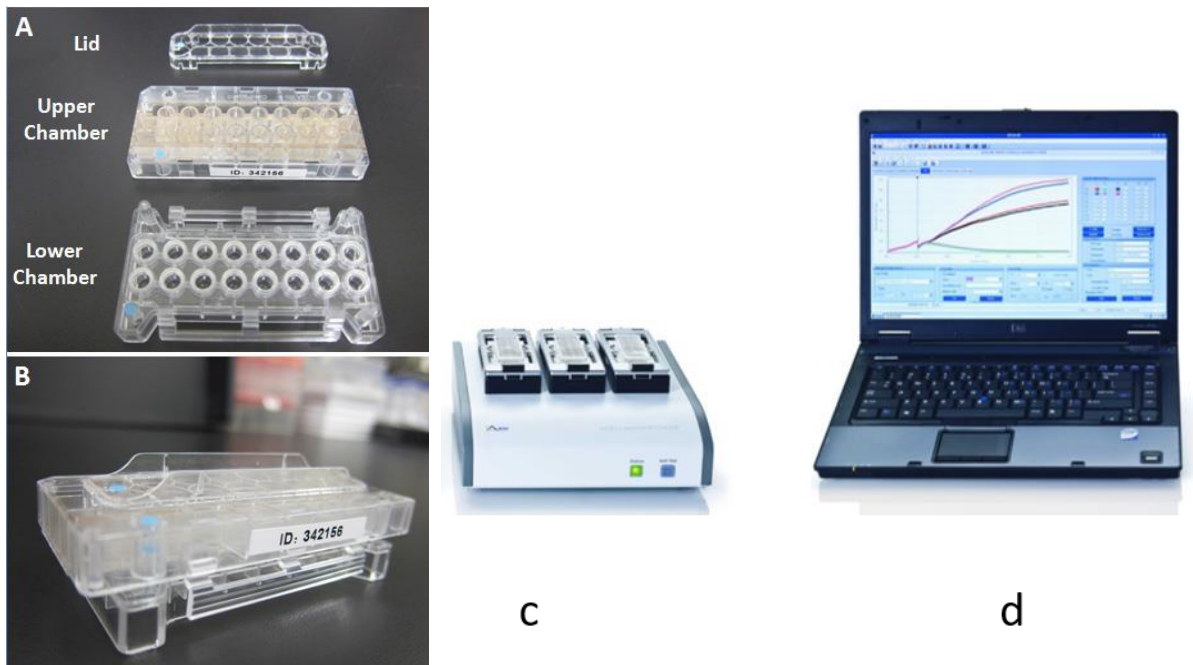
Figure 4. xCELLigence RTCA DP instrument a. CIM plate compartments, **b**. Assembled CIM plate, **c**. Dual-plate (DP) instrument and **d**. Workstation adopted from CIM protocol.

6.5.14. Immunohistochemistry

Immunohistochemistry is the widely used immunostaining technique that differentially stain the protein (antigen) of interest by using specific antibody in tissue sections (139, 140). Immunohistochemistry technique was performed to detect cancer associated fibroblasts (CAFs) in mouse model OSCC tongue sections using anti-α-SMA antibody (1:500) with 1.5% goat serum. Tumors were developed in mouse tongues by injecting 10,000 cells of different construct of AT84-uPAR and AT84-EV cells in different groups of mouse tongue tissue (anterior) as described elsewhere (38). A total of 47 mouse tongue tumors sections from AT84 cells and 10 section from each xenographts and carcinogen induced tongue tumors were immune-stained according to the IHC protocol.

IHC was performed in Zn-fixed paraffin imbedded tongue tissue sections placed on plus adhesion slides. The slides were kept in the heating cabinet for three hours or overnight for tissue sections attached well to the slide. The immunostaining procedure was started with deparaffinization and rehydration process as follows: 2 baths in xylene each for 10 minutes followed by 2 baths in absolute ethanol (100%) each for 5 minutes and then, 2 baths in 96% ethanol each for 5 minutes. Finally, the slides were bathed with deionized water for 5 minutes. Then, the rehydrated tissue sections were removed from the water bath, wiped with gauze paper and incubated for 10 minutes at RT in wet chamber with 1-2 drops of peroxidase block. Peroxidase block was added to inhibit endogenous non-specific background staining. After 3x bath with 1x PBS (5 minutes per bath), 60 µl of the blocking buffer (1.5% goat serum) was added in each section and incubated at RT for 20 minutes in wet chamber to inhibits the non-specific antibody binding. Then, 60 µl of diluted rabbit anti mouse-α-SMA antibody with blocking buffer was added and incubated overnight at 4°C in humid chamber. Two drops of Secondary antibody, polymer-HRP anti-Rabbit peroxidase were applied and incubated for 30 minutes at RT in wet chamber. Sections were washed 3x in PBS each for 5 minutes before adding 2 drops of DAB solution. This was followed by 10 minutes incubation at RT in the hood. DAB solution was prepared by mixing 2 drops of DAB chromogen with 1 ml DAB substrate. DAB solution was washed using Milli-Q water and the substrate was neutralized with hypochlorite. Sections were counterstained with hematoxylin for 30 seconds followed by washing using deionized water. Scotts solution was applied for 15

seconds for blueing nuclear chromatin and nuclear membrane, and to reduce the detachment of tissue sections from glass slides. The sections were washed in running water for couple of minutes. Then, the sections were dehydrated successively in 2 baths of 96% ethanol, 2 baths of 100% ethanol and 2 baths of xylene, each for 2 minutes. The sections were mounted with DPX Mountant and covered with appropriate size cover slips and kept in the hood to dry before visualized under light microscope. The imaging of the immuno-stained sections was done using LAS software. Online Immuno-ratio analysis software was used to analyze the amount of α-SMA[+] CAFs. The application analyzes online the percentage of DAB stained over hematoxylin stained nuclear region of the given immune-stained tissue section image (DAB/nuclear area percentage). Three images (20x magnification) of different regions per sections were used for the analysis.

6.5.15. Statistical Analysis

GraphPad Prism version 5 software was used for the statistical analysis. All results are presented as Mean + standard deviation and comparisons between treatment groups were performed using t-test (unpaired) and One- way analysis of variance (ANOVA). P value < 0.05 was considered as indicator of statistical significance difference.

7. Results

7.1. Medium optimization for activation studies

Cell culture media are designed for the growth and maintenance of mammalian cells. Although different media are available, selection is made based on the demands of the cells under study. Most of the Flp-In 3T3 cells died after 72 hours of culturing in SFM. However, the 10% FBS in the DMEM induced proliferation of cells, which made it difficult for us to study the differentiation of the cells. Hence, medium optimization was performed to find a condition in which Flp-In 3T3 cells survived for 72 hours. Two different culture media, DMEM and RPMI, with different supplements were tested. Media supplements used were ITS, 0.1% FBS, 0.1% FBS + ITS, 0.5% FBS, 0.5% FBS + ITS, 2% FBS and 2% FBS + ITS. Triton X-100 was used as a negative control, while 10% FBS supplement was used as positive control for cells survival. DMEM with 10% FBS is the certified growth medium for Flp-In 3T3 cells.

The viability of Flp-In 3T3 cells in DMEM with 10% FBS was considered a positive control (100% viable, Appendix 11.1). RPMI and DMEM showed comparable survival support (Fig. 5a-c). Better viability was seen in media supplemented with FBS and ITS compared to SFM for all time points (Fig. 5a-c). Medium containing 2% FBS and 2% FBS + ITS induced higher level of viability than the positive controls at 24 hours indicating high level of unwanted proliferation (Appendix 11.1). At 72 hours, both media containing 0.5% FBS + ITS resulted in more than 50% viability compared to the positive control (Fig. 5c). AT84 cells thrive in RPMI, hence, based on these results, RPMI with 0.5% FBS + ITS was selected for activation of Flp-In 3T3 cells and preparation of CMs.

b

48 hrs

c

72 hrs
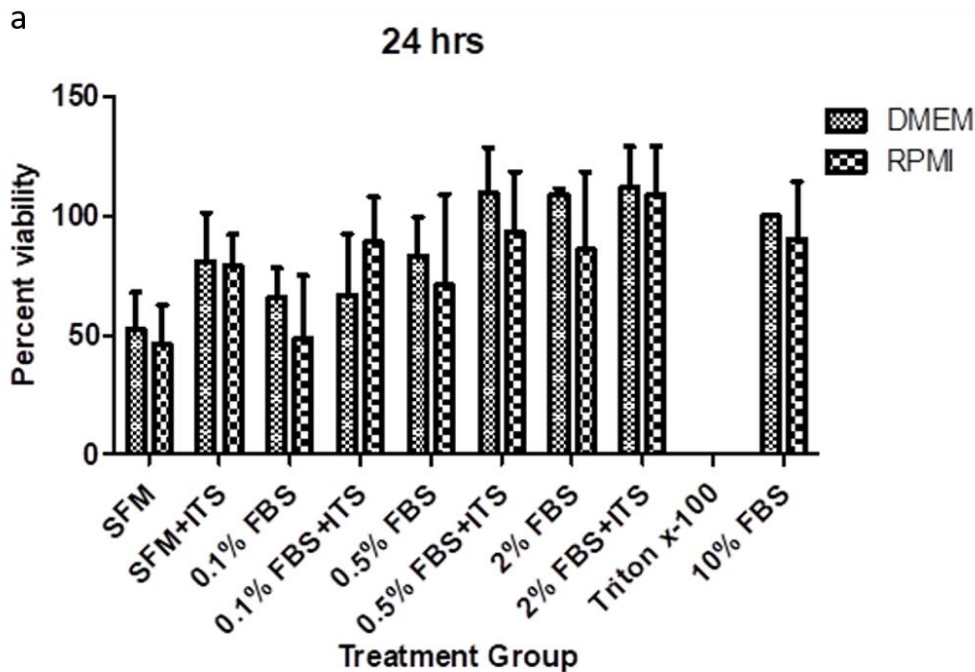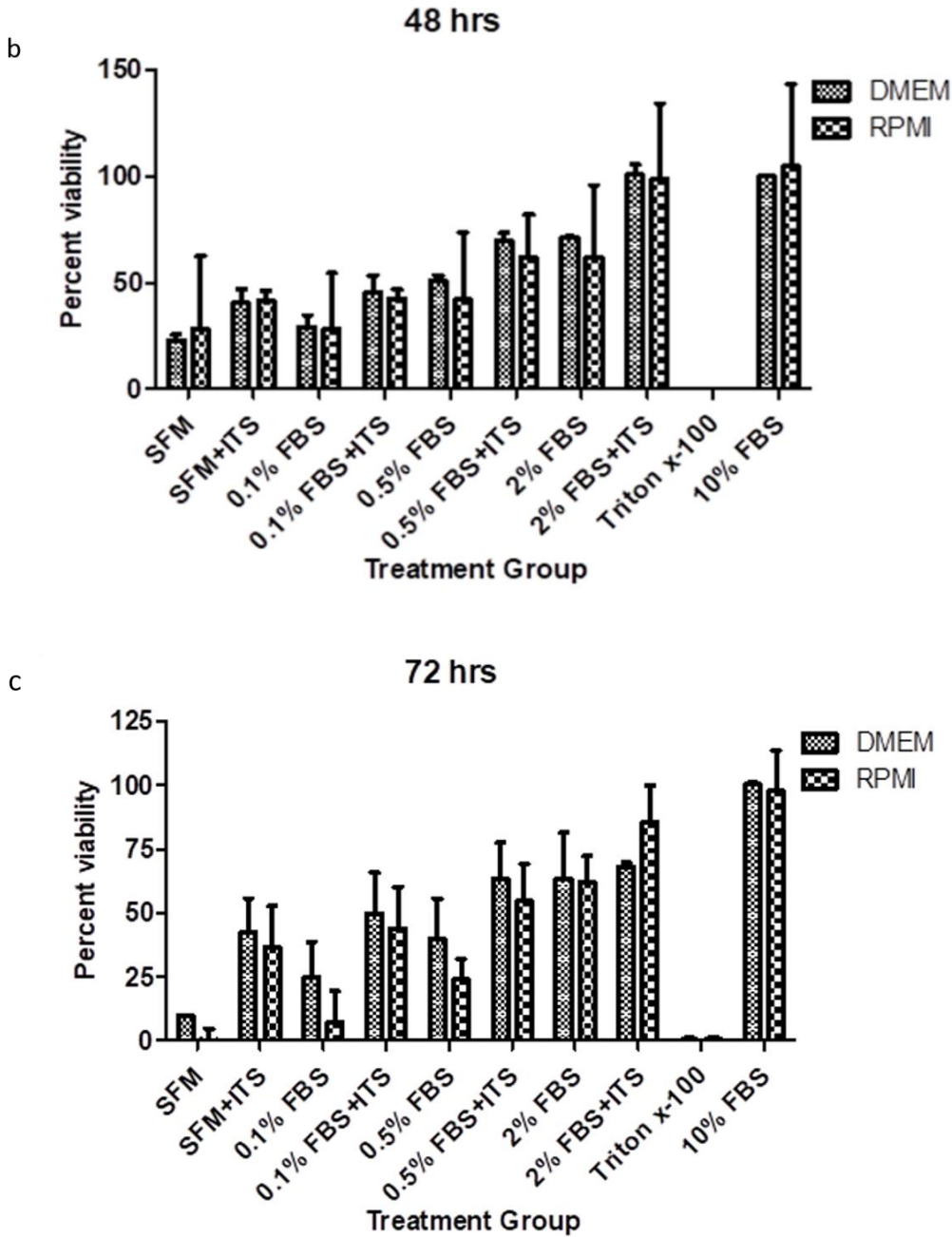
Figure 5: Media optimization and viability percentage of cells*. The OD value was measured at 490 nm at 24, 48 and 72 hours of culture. Viability percentage of cells was calculated based on DMEM with 10% FBS, which was considered supporting 100% viability. The experiment was performed three times with three technical replicates. The relative viability percentage at **a**. 24 hours, **b**. 48 hours and **c**. 72 hours of culture. SFM- Serum free media, ITS- Insulin transferrin selenite, FBS- Fetal bovine serum, DMEM- Dulbecco's modified Eagle medium and RPMI- Rosewell park memorial institute.*
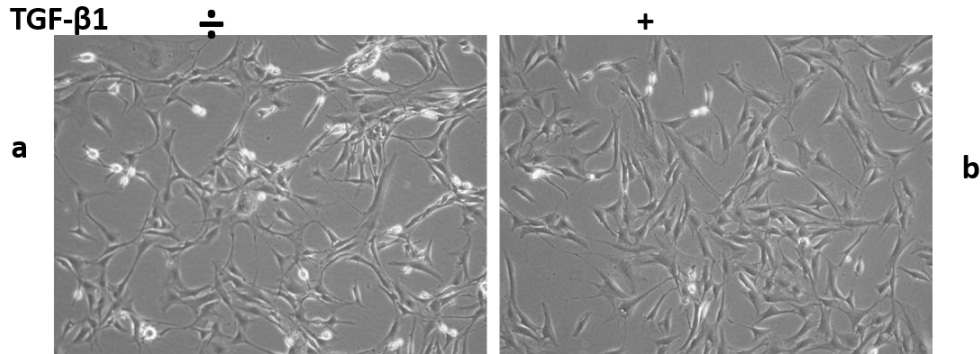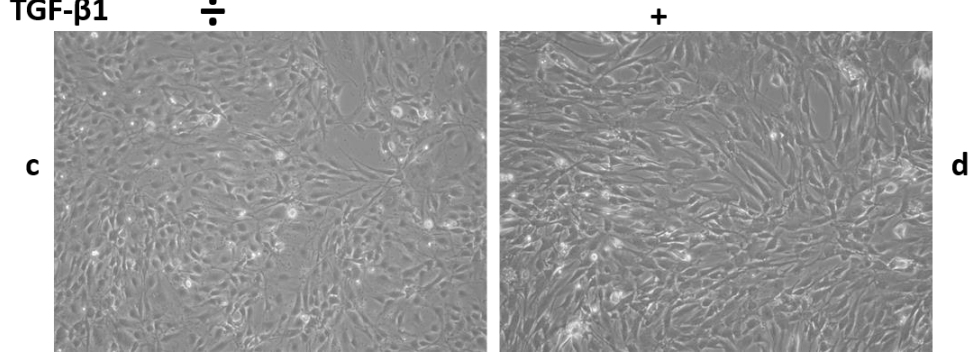
7.2. Flp-In 3T3 cells activation

7.2.1. Activation of Flp-In 3T3 cells by TGF-β1

Here, the aim was to activate the Flp-In 3T3 cells using TGF-β1 in the optimized medium (RPMI with 0.5% FBS + ITS) for 72 hours. Flp-In 3T3 cells were treated with TGF-β1 (2 ng/ml) or left untreated (negative control). Flp-In 3T3 cells treated with TGF-β1 for 72 hours demonstrated morphological change compared with 24 hours treated cells and controls (Fig.6a-d). Activated fibroblasts have a characteristic appearance of stretched or extended cytoplasm due to increased expression of cytoskeletal proteins (e.g. α-SMA and vimentin). In addition, the expression of α-SMA (42 KDa) was analyzed at 24, 48 and 72 hours using western blot analysis (Appendix 11.2). No significance difference in α-SMA expression was seen at 24 hours. However, a significantly increase α-SMA expression was found at 48 hours (p=0.03) and 72 hours (p=0.0007) in TGF-β1 treated cells compared with the control cells (Fig. 6e). To conclude, Flp-In 3T3 cells can be artificially activated through TGF-β1 treatment *in vitro*.

24 hours

TGF-β1　　÷　　　　　　　　　+

a　　　　　　　　　　　　　　　　　　　　b

72 hours

TGF-β1　　÷　　　　　　　　　+

c　　　　　　　　　　　　　　　　　　　　d

e

| 24 hr | 72hr | 48 hr | 72+24hr | 72 hr | 48hr |

÷TGF-β +TGF-β ÷TGF-β +TGF-β

α-SMA

β-Actin

α-Tubilin

f

÷TGFβ
+TGFβ

*p=0.03

***p=0.0007

Expression of α-SMA

30000

20000

10000

0

24 hrs   48 hrs   72 hrs

Treatment and duration of activation
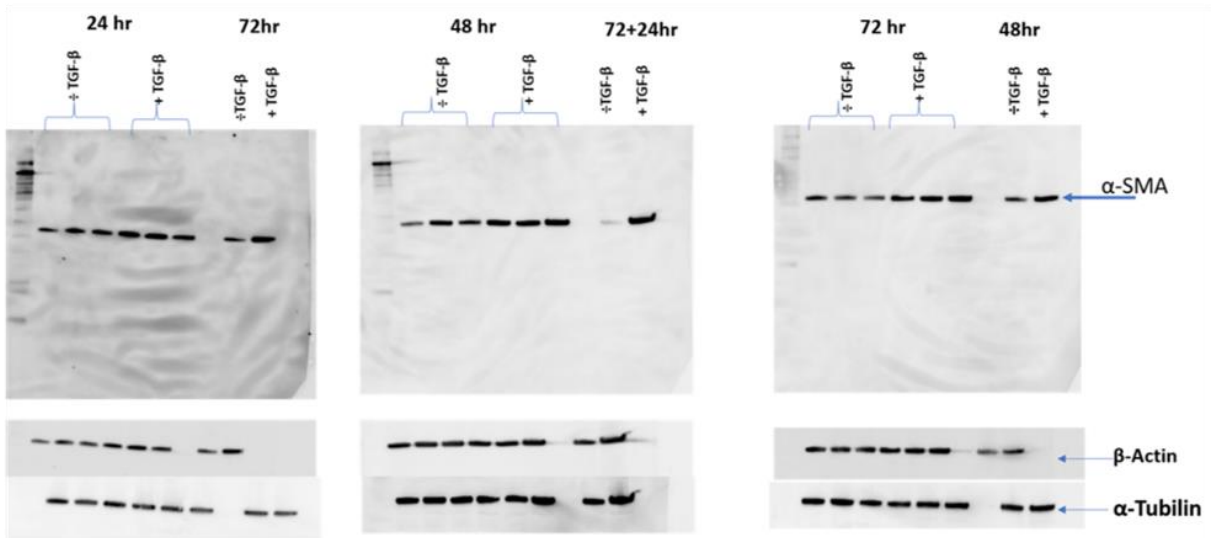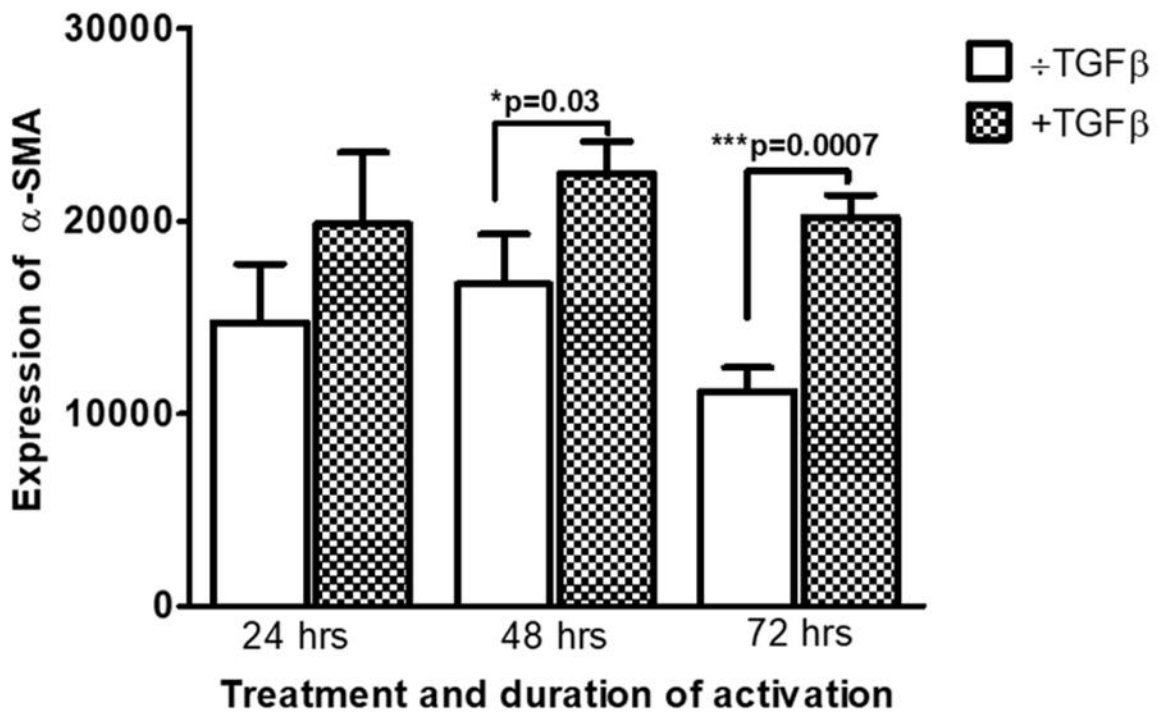
*Figure 6. **Morphological change and α-SMA protein expression in TGF-β1 treated and untreated Flp-In 3T3 cells.** Morphological change was observed in Flp-In 3T3 cells between treatment groups. **a**. 24 hours with-out TGF-β1, **b**. 24 hours with TGF-β1, **c**. 72 hours with-out TGF-β1 and **d**-72 hours with TGF-β1 (10x magnification). **e**. Western blot showing α-SMA protein expression in Flp-In 3T3 cells. Cells were seeded in 12 well plates in RPMI containing 0.5% FBS + ITS (1:100) ±TGF-β1 (2 ng/ml). Both, β- Actin and α-Tubulin were used for loading control. **f**. Graph showing the difference in expression of α-SMA in activated and non-activated Flp-In 3T3 cells. Each time point was performed once in three technical replicates. Significant difference in the expression of α-SMA is indicated by '*' and the degree of significance is indicated by number of '*'. Hence, * is when P= 0.05-0.01, ** P=0.01-0.005 and *** P< 0.005.*

7.2.2. uPAR expression in AT84 cells

Different studies have shown increased expression of uPAR in metastatic cancers (133, 141-143). The AT84 cells used for the following experiments were made to stably express uPAR or an empty vector (EV) as a control (38, 133). Cell lysate were harvested and analyzed for the presence of glycosylated and De-glycosylated uPAR (Fig. 7). As seen in figure 7, AT84-EV cells are uPAR negative, while AT84-uPAR cells overexpress uPAR. As also previously shown (133), when cells are cultured in 10% FBS, most uPAR present as DIIDIII (Fig. 7).
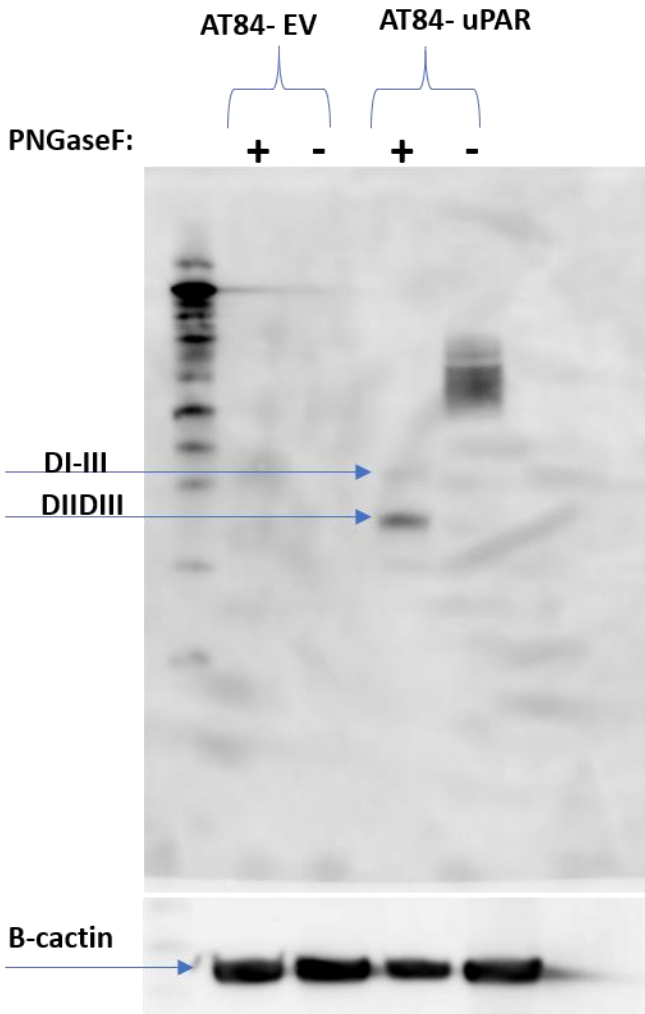
Figure 7. The constitutive expression of uPAR in AT84 cells. *Cells were cultured in 10% FBS supplemented RPMI. De-glycosylated (+) and non-de-glycosylated (-) AT84-uPAR and AT84-EV cell lysates were analyzed for the expression of uPAR using western blot. AT84-uPAR cells expressed uPAR, while AT84-EV did not. The de-glycosylated AT84-uPAR cells lysate showed both the cleaved DIIDIII (26 KDa) and the full-length DI-III (36 KDa) uPAR. The glycosylated uPAR was detected at around 55-60KDa.*

7.2.3. Activation of Flp-In 3T3 cells by CM-uPAR and CM-EV

As demonstrated in the above section, the overexpression of uPAR in AT84-uPAR cells may induce the cells to secret soluble factors that may activate fibroblasts. To evaluate this hypothesis, CMs, CM-uPAR and CM-EV, were prepared and used to activate fibroblasts. Flp-In 3T3 cells were treated with CM-uPAR and CM-EV for 72 hours to see if soluble factors in the CMs induce activation. Since these CMs are from proliferating cancer cells, the CMs might be nutrient depleted and hence, the CMs were mixed with fresh medium in 1: 2 ratio and refreshed every 24

hours during the treatment. Both CMs induced lower expression of α-SMA compared to the negative control (supplemented RPMI medium) (Fig. 8a). No difference in the expression of α-SMA was observed in Flp-In 3T3 cells treated either with CM-uPAR and CM- EV (Fig. 8b). Therefore, these conditions did not activate AT84 cells. Band quantification data is presented appendix (11.3).
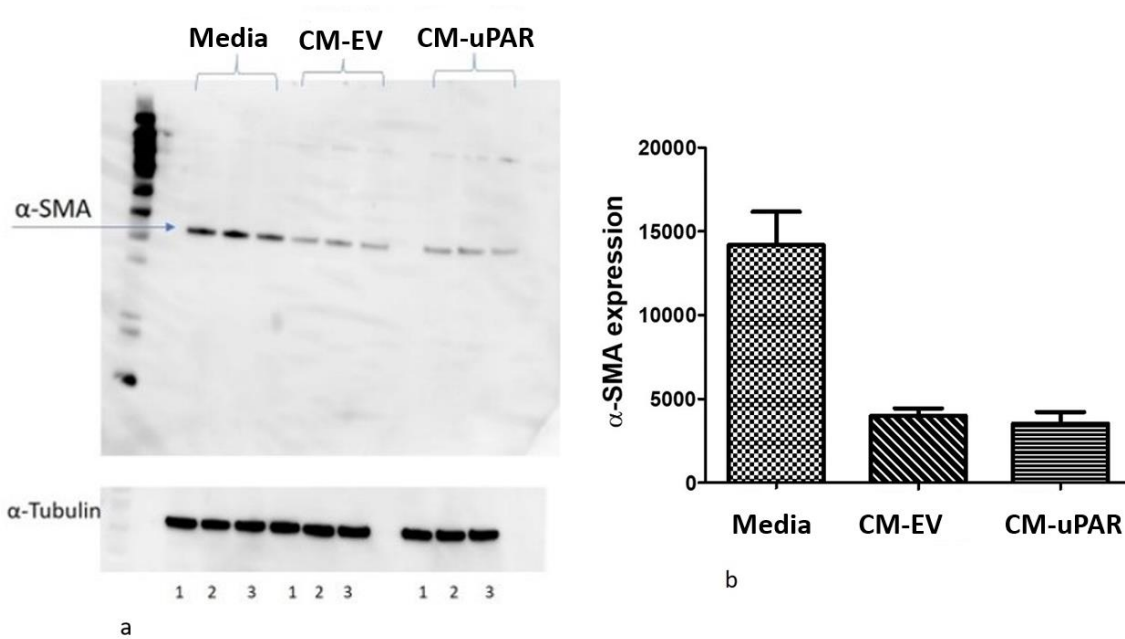
Figure 8. CM-EV and CM-uPAR did not activate *Flp-In 3T3 cells.* *Cells were cultured in RPMI supplemented with 0.5% FBS and ITS (1:100), CM-EV and CM-uPAR for 72 hours. **a**. Representative western blot showing α-SMA expression in control and CMs treated Flp-In 3T3 cells. For loading control, membranes were stripped and blocked using 5% low-fat milk, and re-probed for α-Tubulin. **b**. The band intensity of α-SMA protein expression was quantified using ImageJ software. The experiment was performed twice with three technical replicates.*

7.2.4. CM from TGF-β1 activated fibroblasts induced high amount of full-length uPAR

In this study, we aimed to see the effect of CMs from activated and non-activated fibroblasts on uPAR cleavage. AT84-uPAR cells treated with CM-Flp⁺ exhibited higher amounts of full-length uPAR (DI-III) than AT84-uPAR cells treated with CM-Flp⁺ (Fig. 9a). The quantification of uPAR band intensity confirmed that AT84-uPAR cells treated with CM-Flp⁺ had significantly higher (p=0.0005)

uPAR ratio (DI-III/DII-III) than the AT84-uPAR cells treated with CM-Flp$^{\div}$ (Fig. 9b). (Band quantification data is presented in appendix 11.4)
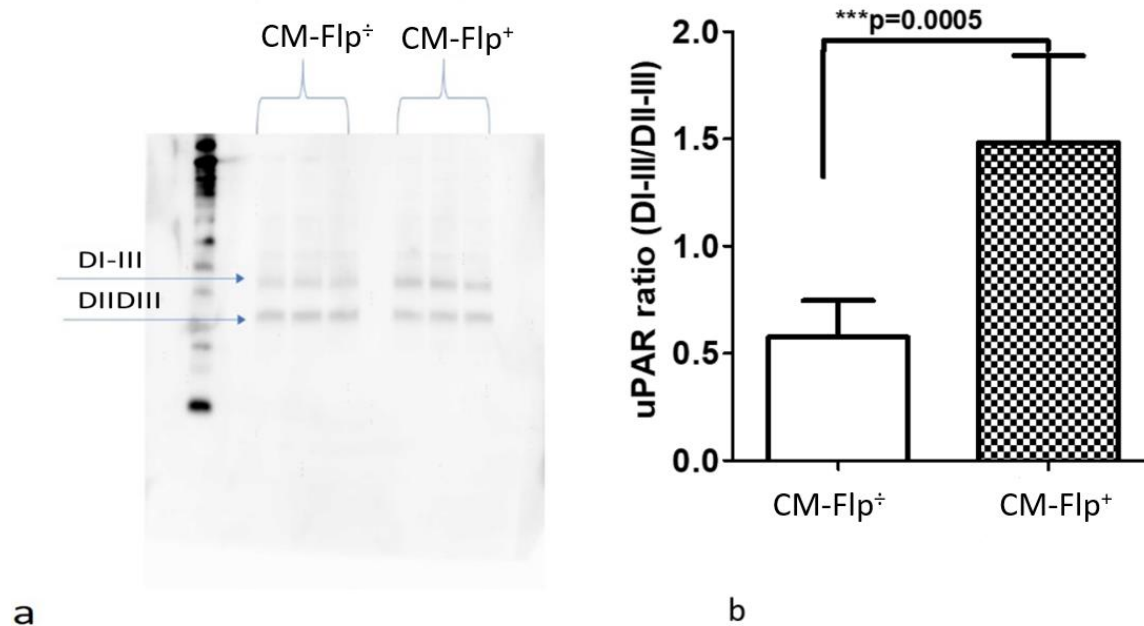
Figure 9. uPAR expression and cleavage. a. *Western blot showing expression and cleavage of uPAR using CM-Flp$^{\div}$ and CM-Flp^{+}. The first 3 lanes are loaded with AT84-uPAR cells treated with CM-Flp$^{\div}$ and the last three lanes are AT84-uPAR cells treated with CM-Flp^{+}.* ***b.*** *The quantification of uPAR ratio (DI-III/DIIDIII) in AT84-uPAR cells, where the full-length uPAR is highly (P=0.0005) expressed in CM-Flp^{+} treated cells. The experiment was performed twice with three technical replicates. Significant difference in the expression of uPAR cleavage ratio is indicated by '*' and the degree of significance is indicated by number of '*'. Hence, * is when P= 0.05-0.01, ** P=0.01-0.005 and *** P< 0.005.*

7.4. Detection of hydrolytic enzymes in the conditioned media

Based on the results in Flp-In 3T3 cells activation and uPAR cleavage regulation, we aimed to determine the soluble factors (hydrolytic enzymes) present in condition media harvested from each experiment.

7.4.1. Zymography results of CM-Flp$^{\div}$, CM-Flp^{+}, CM-Flp$^{\div}$-uPAR and CM-Flp^{+}-uPAR

Gelatin and gelatin-plasminogen zymography analysis of the above CMs revealed the presence of hydrolytic enzymes that might have a role in uPAR cleavage (Fig. 10a and b). The hydrolytic

enzymes identified were MMP2 (72 KDa), MMP9 (93 KDa) and muPA (55 KDa) (Fig. 10a and b). Unknown band was also detected in gelatin-plasminogen zymography indicating that the presence of additional protease enzymes (Fig. 10b). TGF-β1 treated Flp-In 3T3 cells CM, CM-Flp⁺, displayed increased secretion of MMP2 (Fig.10a) and low uPA (Fig. 10b) compared to untreated cells.
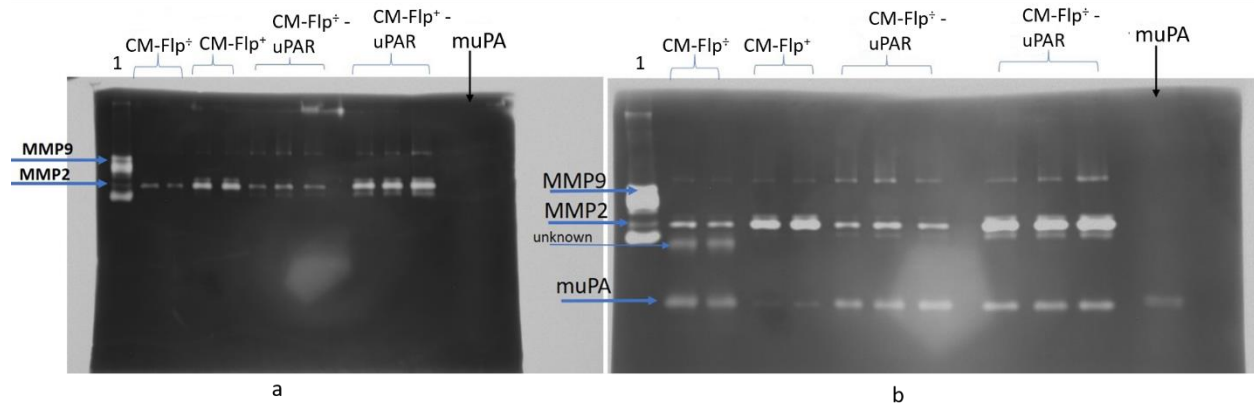
Figure 10. *Gelatin and Gelatin-Plasminogen Zymography of CM-Flp⁺, CM-Flp⁺, CM-Flp⁺-uPAR and CM-Flp⁺-uPAR. Lane 1 is Human-MMP2/MMP9, lanes labeled muPA are positive controls, while other lanes are loaded with samples as labeled in the figure. The same samples with technical replicates were loaded in **a.** gelatin and **b.** gelatin-plasminogen. Three in-gel zymography were performed in conditioned media harvested from three experiments.*

No difference in uPA activity was observed when AT84-uPAR cells were treated with CM-Flp⁺ or CM-Flp⁺, while higher activity of MMP2 was observed in CM-Flp⁺ treated cells than CM-Flp⁺ treated cells. Higher MMP9 activity was observed in CM-Flp⁺-uPAR and CM-Flp⁺-uPAR than in CM-Flp⁺ or CM-Flp⁺. However, from the figure, MMP9 activity was unaffected in both CMs, i.e. CM-Flp⁺-uPAR and CM-Flp⁺-uPAR (Fig. 10a).

7.4.2. Zymography results of CM-uPAR, CM-EV, CM-uPAR-Flp and CM-EV-Flp

Gelatin and gelatin-plasminogen zymography were used to determine the presence of proteases in CM-uPAR and CM-EV. MMP2 activity was not detected from both CMs, CM-EV and CM-uPAR (Fig.11a and b) while its activity was detected in both CM-uPAR-Flp and CM-EV-Flp. In addition, more uPA was found in CM-uPAR, CM-uPAR-Flp and CM-EV-Flp than the conditioned medium harvested from control Flp-In 3T3 cells (CM-Ctrl) cultured and CM-EV. Difference in the amount

of MMP2 was not detected in CM-uPAR-Flp and CM-EV-Flp, while it was found at a higher amount in CM-Ctrl. Mouse plasmin was not detected in any of the samples whereas MMP9 activity was seen (Fig. 11a and 11b).
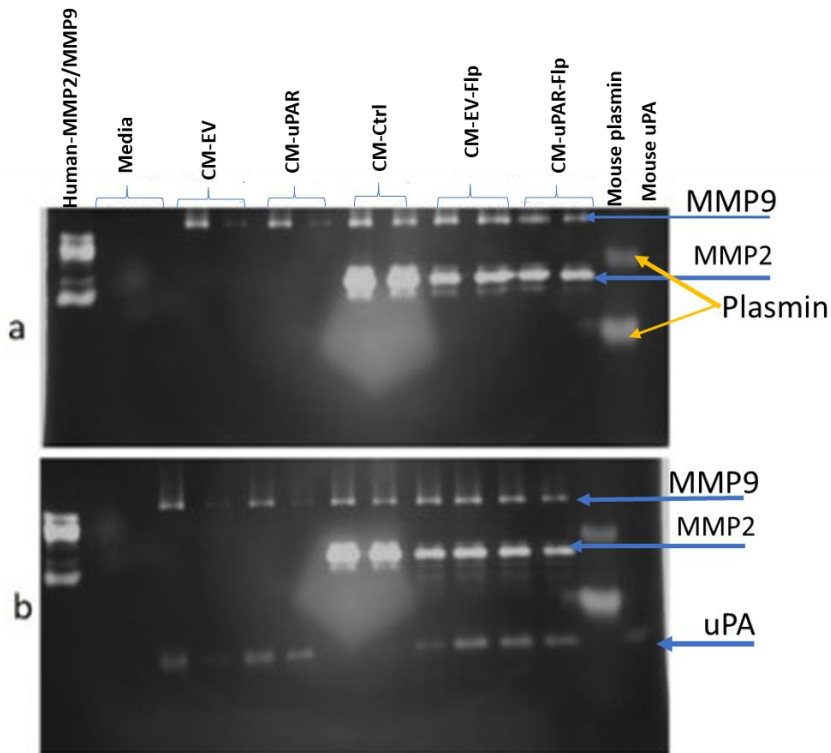
Figure 11. Analysis of CM-uPAR, CM-EV, CM-uPAR-Flp and CM-EV-Flp by gelatin and gelatin-plasminogen zymography. a. Gelatin zymography showing the MMP2 and MMP9 in the above CMs (the blue and yellow arrows show the presence of hydrolytic proteases). b. Gelatin-plasminogen gel showing the presence of MMP2, MMP9 and uPA in the different CMs. Similar samples were loaded in corresponding wells of both gelatin and gelatin-plasminogen gels in duplicate. Three in-gel zymography were performed in conditioned media harvested from three experiments. Higher MMP2 expression and no uPA were found in CM-Ctr.

7.5. PAI-1 detection in the conditioned media

PAI-1 is a known inhibitor of uPA (144). AT84-uPAR cells were treated with CMs from activated and non-activated Flp-In 3T3 cells to study uPAR cleavage regulation. Western blot results of AT84-uPAR cells treated with CM-Flp[+] showed more-full length uPAR than cleaved uPAR (DII-DIII) (Fig. 9a). Hence, we hypothesized that PAI-1 might have inhibited the activity of uPA in AT84-

uPAR cells treated with CM-Flp$^+$ (Fig. 10b). Interestingly, differences in the amount of PAI-1 was observed in the different CMs using western blot analysis (Fig. 12a and b). Higher amount of PAI-1 was in CM-Flp$^+$, while it was undetected in CM-Flp$^\div$. Except in the negative control medium (media, Fig. 12b), all the CMs harvested from Flp-3T3 cells, CM-uPAR-Flp and CM-EV-Flp, had similar level of PAI-1 (Fig. 12b).
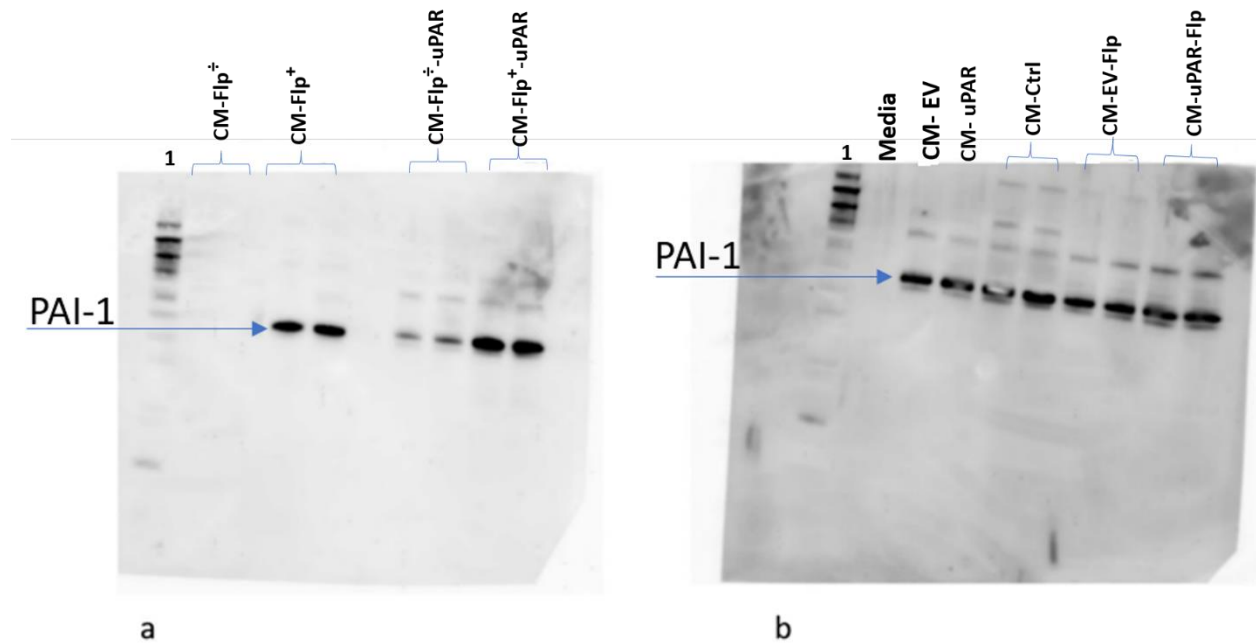
Figure 12. ***Western blot analysis of PAI-1 in CMs. a.*** *The detection of PAI-1 (45KDa) in CM-Flp$^\div$, CM-Flp$^+$, CM-Flp$^\div$-uPAR and CM-Flp$^+$-uPAR **b**. PAI-1 in media, CM-EV, CM-uPAR, CM-Ctrl, CM-EV-Flp and CM-uPAR-Flp.*

7.6. Soluble uPAR (suPAR) does not increase migration of Flp-In 3T3 cells

The cell migration assay was performed to determine whether different soluble factors could function as chemoattractant for Flp-In 3T3 cells. As described in the introduction, cell bound uPAR can be cleaved into DI, DIIDIII and DI-III fragments by the action of protease enzymes (such as uPA). The DI-III fragment is also called soluble uPAR (suPAR). In this assay, SFM (DMEM) and different supplements were used to study their chemoattractant effect on Flp-In 3T3 cells. The medium supplements used were 10% FBS, CM-uPAR, CM-EV, 10 ng/ml suPAR, 500 ng/ml suPAR and 10 μg/ml suPAR. DMEM supplemented with 10% FBS showed the highest cell index

suggesting that it has more chemoattractant for the Flp-In 3T3 cells. Although increased concentration of suPAR was found to be associated with a slight increase in cell migration index, this increase was not statically significant (p>0.05) (Fig. 13). In conclusion, suPAR does not significantly increase Flp-In 3T3 cells migration under these conditions.
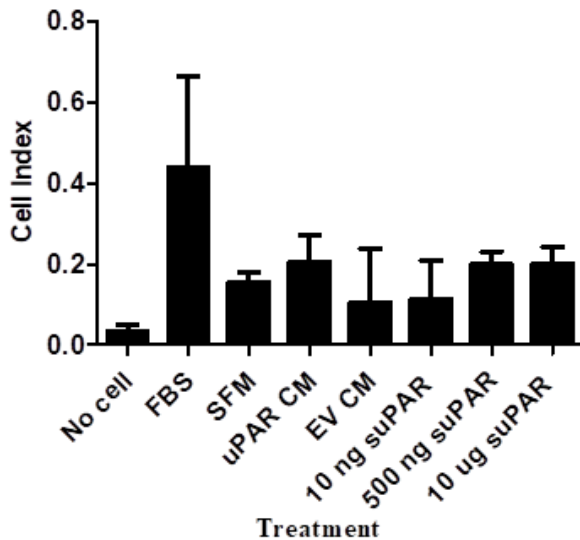
Figure 13. Migration of Flp-In 3T3 cells in response to suPAR and other media supplements. *Flp-In 3T3 cells, 2000 cells per well, were seeded in CIM plate wells except in wells labeled with no cells. Different media supplements were used to determine their chemoattractant effect on Flp-In 3T3 cells in 12 hours culture. No cell – CIM plate wells without cells, FBS-fetal bovine serum, SFM-serum free media, uPAR-CM- urokinase receptor condition media, EV CM-Empty vector condition media and SuPAR-soluble uPAR.*

7.7. Expression of α-SMA in CAFs

Poor prognostic significance of CAFs has been described in various types of cancers (42, 145). In this experiment, anti- α-SMA antibody was used to detect CAFs in sections of mouse tongue OSCC. AT84-uPAR and AT84-EV cells, 10,000 cells from each construct, were injected in different groups of mouse tongue tissue (anterior) and grew into tumors, as described elsewhere (38). CAF score analysis was performed using immunorato application in mouse tongue tumor sections to study whether CAFs infiltration correlated with expression uPAR on cancer cells. Preinjected uPAR expression of each construct and *in vivo* uPAR expression of developed mouse tongue tumors is depicted in appendix (11.5a-c) (38). α-SMA expression was restricted to smooth muscle cells and glands (base of tongue) in normal tongue tissues (Fig. 14a and b). The expression of α-

SMA was significantly higher (P=0.0018) in tongue tumor sections from high uPAR expressing cells injected and grown into tongue tumors (uPAR2-2) than in tumors from lower uPAR expressing cells (uPAR2-3) (Fig 14c and d). Control cells containing only an empty vector (EV3 and EV4 cells) also showed varying CAF scores. EV4 showed significantly lower amount of CAF infiltration (P=0.019) compared to high uPAR (uPAR2-2). CAF score quantification data is presented in appendix (11.6). Although α-SMA expressing CAFs were seen in tongue tumor sections, other cells including AT84 cells, immune cells and smooth muscle cells lining the blood vessels were also found expressing α-SMA (Fig.14c-d). In conclusion, there was a relatively high CAFs infiltration with respect to high uPAR expression in grown OSCC tongue tumors.
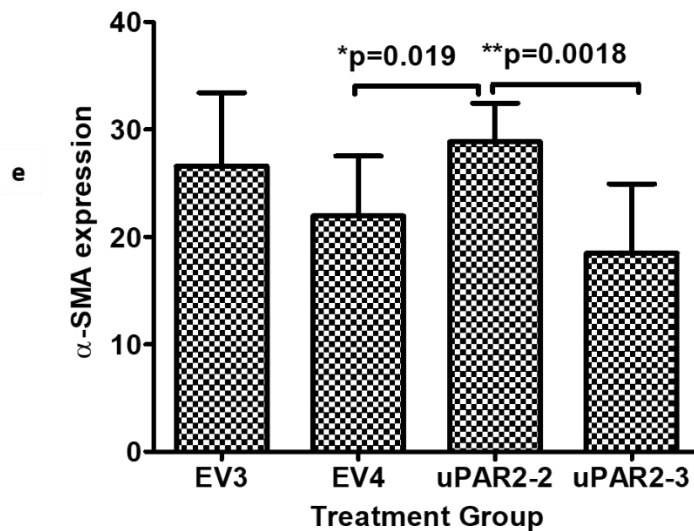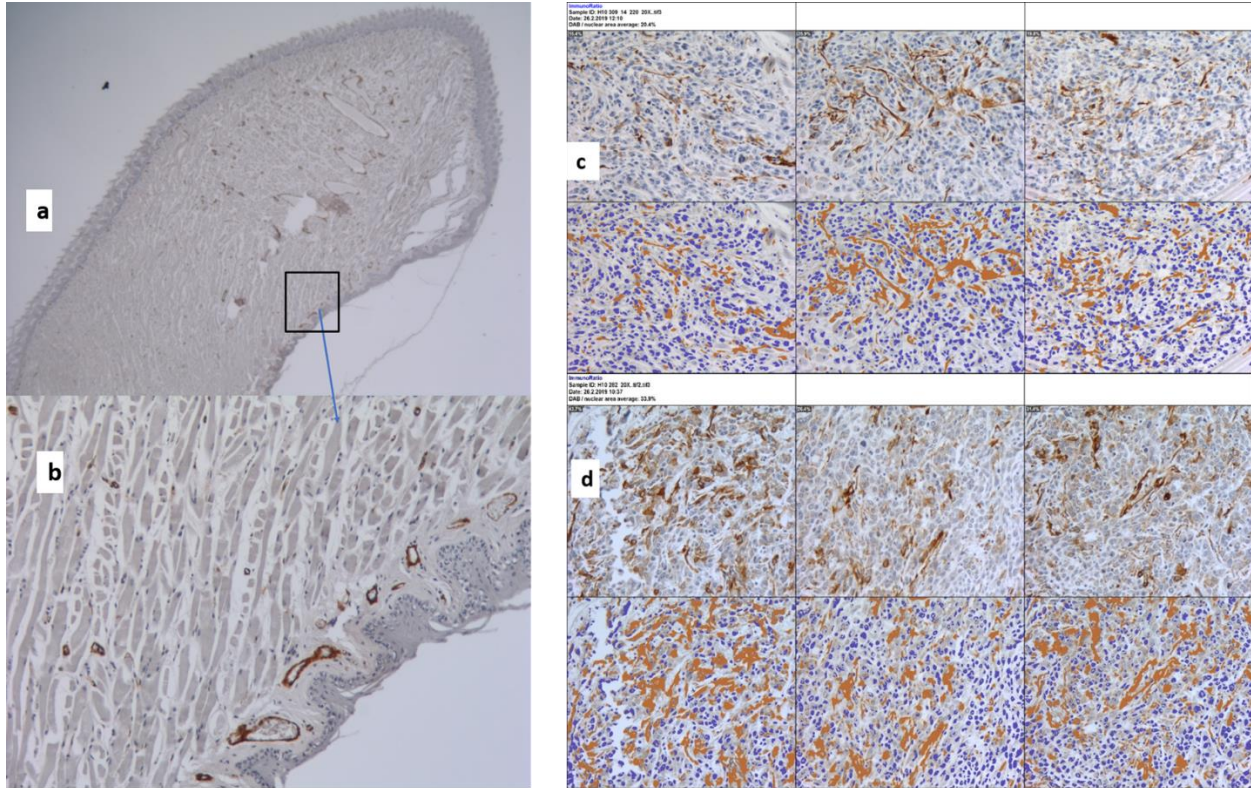
Figure 14. Relative α-SMA score in mouse tongue models of OSCC. a and b. *Non-injected normal mouse tongue tissue (negative control) (**a, 1.6x**) that shows blood vessel smooth muscle cells (**b, 10x**) expressing α-SMA. **c.** Immune-ratio analyzed using ImageJ software depicting low CAF score in tongue tumor sections in uPAR2-3 and **d.** high uPAR expressing cells grown tongue tumor section (uPAR2-2) shows relatively higher CAF score to uPAR2-3 and EV4. **e.** Relative α-SMA score in mouse tongue tumors sections grown by injecting different uPAR expressing construct of AT84 cells. EV3-low detectable uPAR (N=9), EV4-low detectable uPAR (N=5), uPAR2-2-high uPAR (N=8) and uPAR2-3-low uPAR (N=7) expressing cells grown tongue tumor sections.*

7.8. Detection of CAFs in xenographts and carcinogen induced tongue tumor sections

Xenographts are graphts of tissue from different species of animal transplanted to immunocompromised host. In this experiment, mouse tongue tumors grown from human OSCC cells were used. The aim was to determine whether xenografted human OSCC cells would induced CAFs in mouse tongues. Immunohistochemically stained tumor sections demonstrated the presence of α-SMA expressing CAFs, but also α-SMA positive epithelial cells (Fig. 15a and b).
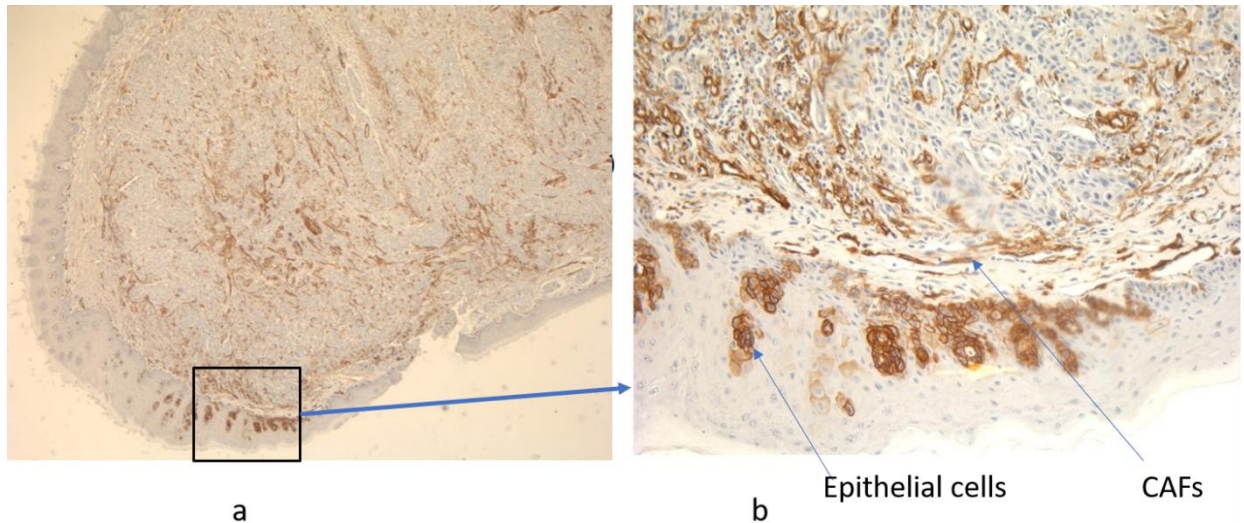
Figure 15. IHC staining of α-SMA in xenographt tumors. *Human OSCC cells injected to mouse tongue showed the growth of xenographt tumor infiltrated with α-SMA⁺ CAFs. Figure **a** and **b** showed tongue tumor with 4x and 40x magnification of the indicated area (rectangular area), respectively.*

4-nitroquinoline-1 oxide (4NQO1) is a known carcinogen that bind to nucleic acid (146), resembling the mutagenic action of tobacco. To induce oral cancer, mice were supplied with 4NQO1 in the drinking water. 4NQO1 induced tongue tumor sections were IHC stained to detect α-SMA⁺ CAFs. These tongue tumors were harvested at early time point in OSCC development. The aim of the experiment was therefore to determine whether α-SMA positive CAFs could be detected in these tongue tumors. Accordingly, α-SMA expressing cells were observed in different tongue tumor lesions including in papilloma (Fig. 16a) and an early stage oral lesion (Fig. 16b). Few α-SMA positive CAFs were observed in these early stage tumors, however, many epithelial cells were positively stained for α-SMA.
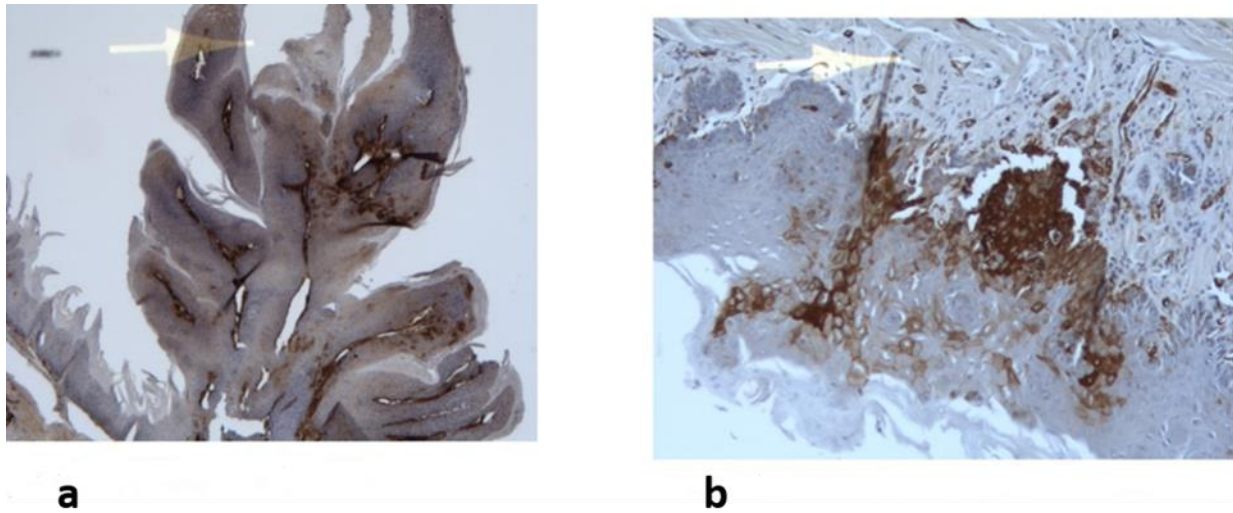
Figure 16. IHC staining of α -SMA in mouse carcinogen-induced tongue tumor. *Tongue tumor sections (N=10) were IHC stained using α-SMA antibody. α-SMA positive cells appeared brown counterstained with hematoxylin.* ***a.*** *Papilloma located on the dorsal surface of tongue.* ***b.*** *Early stage lesions at the epithelial cell lining of the lateral side of tongue section.*

8. Discussion

8.1. Viability assay for media optimization

Culture media play a major role in providing nutrients so that cells can survive and grow *in vitro*. Although different cells have different nutrient requirements, culture media generally contain glucose, amino acids, vitamins and salts (147, 148). However, supplementing the basal media with different growth factors and serum usually improves the longevity of cultured cells (149). The aim of this particular study was to find a culture medium that support survival, but with minimal proliferation. Hence, viability assay was performed to find an optimal culturing condition for Flp-In 3T3 cells. FBS is an ill-defined medium supplement that contains different growth factors with varying concentration. At higher concentration, FBS induces cell proliferation (150). We assumed that low percentage of FBS with 1% ITS can promote the *in vitro* viability of cells used in this study. Other studies have demonstrated better viability of cells with 1% ITS as a baseline medium supplement (151-153). Based on visual inspection of the cells (Appendix 11.1a and b) and the MTS experiment result (Fig. 5), RPMI supplemented with 0.5% FBS and ITS (1:100) was chosen as the optimal medium for further studies. This medium was also compatible with the AT84 cells and used in the subsequent experiments (133). The AT84-uPAR cells are highly

proliferating mouse squamous epithelial cancer cells that require a special medium supporting their higher metabolism. RPMI has extra supplementation with biotin, vitamin B12 (co-factor for DNA synthesis and metabolism) and P-amino benzoic acid (PABA), which are not normally found in DMEM.

Although high FBS concentration of the cell culture medium is known to increase the *in vitro* survival of cells, in this experiment the 2% FBS induced proliferation of cells, which is against the optimal condition that we were targeting at. To the contrary, the low FBS concentration, 0.1%, resulted in low viability of cultured cells. Hence, ITS supplementation minimizes the unwanted proliferation of cells and variability that would arise due to high concentration of FBS. The finding that ITS supplementation promotes viability (Fig. 5) is in agreement with a previous study that has reported better viability of cells with ITS than SFM alone (154). In this study, the viability assay was performed without changing the medium for all the time points. Thus, the gradual decrease in the viability of cells with increasing duration in culture might be due to depletion of nutrients in the culture medium. Therefore, during the Flp-In 3T3 activation experiment, we changed the medium once in 24 hours to replenish the nutrient and the activator, TGF-β1. Similarly, low viability was observed in Flp-In 3T3 cells treated with CM-uPAR and CM-EV prepared from AT84 cells, which might be due to depletion of nutrient in CMs. However, upon mixing with fresh medium (one-part fresh medium with two parts of CM) that was supplemented with FBS (0.5%) and ITS (1:100) a better viability was observed, which is in agreement with other investigators (154, 155).

8.2. TGF-β1 activates Flp-In 3T3 cells

CAFs are the main role player in TME for tumor progression (156). In this study, we were interested if we could activate the Flp-In 3T3 cells *in vitro* using TGF-β1. Even though α-SMA is the most commonly described CAF marker, FSP1, FAP, and PDGFR α/β are also used in CAFs detection. These markers are poor prognostic markers (145, 157). The activation status of fibroblasts was demonstrated by analyzing α-SMA expression (Fig.6). TGF-β1 induces transcription of genes that favor fibroblast differentiation (158). Similar to our findings, activation

of vocal cord fibroblasts with TGF-β1 resulted in increased α-SMA and MMP2 expression with a characteristic elongated morphology (159). However, Flp-In 3T3 cells treated with CM-uPAR and CM-EV exhibited low expression of α-SMA (Fig. 4) than the control cells suggesting that factors other than TGF-β1 could be involved in the activation process e.g. direct cell-to-cell contact as described by other investigators (160).

α-SMA expressing CAFs were also observed in mouse tongue tumors grown from OSCC cells, xenographts, grown from injected human OSCC cells (Fig. 14) and 4NQO1 (Fig. 15) induced tongue tumors. The presence of α-SMA expressing fibroblast in tongue tumor sections of human OSCC has also been reported (161). The increased expression of α-SMA⁺ CAFs has also been associated with increased invasiveness and progression of OSCC (162-164).

8.3. Activated fibroblasts regulate uPAR cleavage

uPAR, a three domains anchored receptor, has different functions in normal cell biology and pathological conditions. The presence of all the three domains (DI, DII and DIII) is required for efficient cell adhesion, migration and proliferation (117). The cleavage of uPAR occurs either between DI and DII or at GPI region. Cleavage at GPI region releases a full-length soluble uPAR. Different enzymes are known to induce uPAR cleavage that include for instance uPA, trypsin, chymotrypsin, plasmin, phospholipase C and D (115, 165). Cleavage of uPAR resulted in DI and DIIDIII variant upon uPA binding, where the cell bound cleaved uPAR (DIIDIII) remains without ligand (uPA) binding property (165). The soluble full-length uPAR (suPAR) can also be cleaved with uPA and plasmin (114, 166, 167). In this study, the presence of the full-length uPAR in CM-Flp⁺ treated cells with the presence of high MMP2 showed no association between uPAR cleavage and MMP2 concentration but with uPA. However, the role of MMP2 in the degradation of ECM and activation of growth factors signaling has been documented (168, 169). Further, plasmin was not detected in the study samples suggesting that uPA might induced the uPAR cleavage as reported elsewhere (165). Other investigators have studied the involvement of different MMPs in uPAR cleavage and have found that MMP2 and MMP9 have no role in uPAR cleavage, while the cleavage is associated with MMP12, which is called macrophage elastases and produced by

human macrophages and endothelial cells (113). Therefore, activated fibroblasts regulate uPAR cleavage in cancer cells.

8.4. TGF-β1 activation increases PAI-1 expression

PAI-1 is a known inhibitor of uPA (170). TGF-β1 activation of fibroblasts increases turnover of ECM and expression of PAI-1 in renal T2 epithelial cells and vascular smooth muscle cells (171, 172). Similarly, in this study, activated Flp-In 3T3 cells exhibited increased PAI-1 expression (Fig. 10a), while uPA was hardly detected (Fig. 11) suggesting that PAI-1 might downregulate the uPA activity. However, it has been reported that increased PAI-1 inhibits the uPA dependent activation of MMPs, which degrades collagen, thereby inhibits metastasis (172). In contrary, low concentration of PAI-1 has been shown to induce migratory phenotype of cancer cells by inducing actin cytoskeletal rearrangement (173). In pancreatic metastatic cancer, upregulation of both uPAR and MMP2 expression was observed indicating that activated MMP2 might degrade ECM and promote migration of cells in uPA dependent manner (141).

ECM proteolysis is determinant for the cancer cell migration through the activation of MMP2 and uPA, which activates the plasminogen system. The interaction of TGF-β and PAI-1 in inducting cell migration was described where TGF-β increased the PAI-1expression and then induced significant cell motility (171). Upregulation of PAI-1 expression might induce endocytosis of bound uPA- uPAR through low density lipoprotein receptor-related protein 1 (LRP-1). LRP-1 has been reported having a function of receptor mediated endocytosis (174). The internalized uPA might destined to direct degradation and re-expression of uPAR and LRP-1 might take place to the direction of migration (175-177). Supporting this, our result indicated that the upregulation of PAI-1 expression in TGF-β1 activated Flp-In 3T3 cells might have promoted of full-length uPAR in AT84 cells via inhibiting uPA. A similar findings, increased expression of PAI-1 and uPAR, have also been reported in AT84 cells upon direct TGF-β1 treatment (133). This further indicates a paracrine effect of PAI-1 from activated fibroblast (CAF) in maintaining a functional full-length uPAR in AT84-uPAR cells thereby different uPAR mediated signaling favor the progression of cancer. Therefore, uPAR cleavage was not induced by TGF-β1 mediated activated fibroblasts.

8.5. Soluble uPAR (suPAR) does not increase migration of Flp-In 3T3 cells

High uPAR expression increases the ability of cells to migrate (178). In addition, the cleaved uPAR (DII-III), containing a SRSRY and PRGRY peptides in human and rat, respectively, has been reported to function in chemotaxis and cytoskeletal rearrangement thereby cleaved uPAR facilitates cell migration (179, 180). The cleaved uPAR SRSRY sequence peptide upon interacting with formyl peptide receptors (FPRs), which belongs to the family of G-protein coupled protein receptors, induce ERK signaling that resulted in increased metastasis (181). In this study, even though statistically not significant, increased cell migration was observed with increased recombinant suPAR concentration (10 ng/ml to 10 µg/ml). In addition, the highest migration of Flp-In 3T3 cells was also noticed in 10% FBS supplemented medium (Fig. 12) indicating the involvement of other soluble factors in the serum that favor migration. Similarly, higher but statistically insignificant cell migration index was observed in CM-uPAR treated cells than in CM-EV treated cells (Fig. 12). This might suggest the presence of DII-DIII uPAR variants in CM-uPAR, which has a chemotactic function as it was described by Synnøve et al (133). Binding specificity of suPAR to integrins (α4β1, α6β1, α9β1, and αvβ3) has been reported in Chinese hamster ovary cells (182). Therefore, the suPAR used in our study might also interacted directly with integrins on Flp-in 3T3 cells and induce migration of cells as well.

8.6. uPAR expression enhances in vivo CAFs infiltration in tumor stroma

Hepatocyte growth factor (HGF) secreted by CAFs increase the expression of uPA and uPAR in cancer cells (183). uPAR has been reported to recruitment of hematopoietic stem and progenitor cells in angiogenesis (184). Thus, here we wanted to study the interaction of uPAR and CAFs in different tongue tumor sections using α-SMA expression as a marker for CAFs infiltration. Tumors developed by mouse OSCC cells in mouse tongues appeared localized with boundary formation, while the human OSCC cells, zenographts, developed into invasive characteristic (Appendix 11.7a and b). This difference might be related with the immune system of the mouse models used in the two experiments, syngeneic and nude, respectively. The expression of α-SMA has been reported in normal epithelial cells, cancer cells (185), CAFs and macrophages (186, 187). Similarly,

in this study, the expression of α-SMA was found in cancer cells as well as CAFs in tongue OSCC tumor sections. Increased uPAR expression has been described in many cancers, which in turn indicates poor prognosis (188). uPAR plays a role in cells adhesion with ECM, particularly with vitronectin. Up-regulation of uPAR expression was indicated in induction of EMT that has a role in invasion and metastasis in breast cancer (189). EMT and CAFs have been reported to express α-SMA (38). Similarly, in this study, quantifying α-SMA expressing CAFs was a big challenge as it was expressed by other cells. However, we observed high CAFs infiltration in high uPAR expressing cells injected mouse tongue tumors than no uPAR expressing cells (EV2) and low uPAR expressing cells tumor sections (uPAR2-3) (Fig. 14e). The mouse tongue tumors grown from EV3 cells showed comparable CAFs infiltration with high uPAR, which might be due to the induction of endogenous uPAR expression as it was reported elsewhere (38) (their uPAR expression history depicted in appendix 11.5e). These findings, therefore, collectively indicate that CAFs and uPAR have positive regulatory interaction in the TME.

9. Conclusion and Recommendations

The reactive tumor stroma of many tumors is dominated by activated fibroblasts (CAFs). CAFs via secretion of various growth factors, cytokines, chemokines, and the degradation of extracellular matrix promote tumorigenesis. In the first part of this study, we optimized a medium condition that kept Flp-In 3T3 cells viable for 72 hours with minimal proliferation. This optimal condition was used to create artificial CAFs by activating Flp-In 3T3 cells with TGF-β1. CM was harvested from the artificial CAFs of overnight culture, which supposedly contained different soluble factors that may affect the cleavage of uPAR. AT84 cells overexpressing uPAR were treated with this CM to study the cleavage of uPAR. Whereas analysis of cell lysates from TGF-β1 treated Flp-In cells condition media revealed high amount of full-length with high amount of PAI-1 in CM-Flp⁺. Further, when the CM from TGF-β1 non-activated Flp-In 3T3 cells was used to treat uPAR overexpressing AT84 cells, it induced uPAR cleavage suggesting that the presence of uPA mediated uPAR cleavage. In addition, CM from AT84 cells overexpressing uPAR was used to study if soluble factors released from cancer cells would activate fibroblasts. The result, however, did not support our hypothesis as no difference in α-SMA expression was observed in both CMs harvested from uPAR and EV cells treated Flp-In 3T3 cells. The different experiments in this work resulted in generating the following findings.

✓ RPMI with 0.5% FBS and 1% ITS kept fibroblasts viable for 72 hours with minimal proliferation

✓ TGF- β1 can be used to activate fibroblasts *in vitro* and induce artificial CAFs

✓ Activated fibroblasts (artificial CAFs) produced PAI-1

✓ PAI-1 results in reduced uPA activity

✓ PAI-1 results in less uPAR cleavage and more full-length uPAR

✓ CM from AT84 cells did not activate fibroblasts

✓ suPAR did not induce Flp-In 3T3 cells migration

✓ Tumors expressing more uPAR demonstrated the increased amount of CAFs infiltration

Further study, however, should be done to profile soluble factors present in the CMs using high throughput technique that could help understand better what is happening downstream of TGF-

β1 activation of fibroblasts. Future studies should also aim identifying the mechanism of full-length uPAR expression and uPAR cleavage regulation by activated fibroblasts in AT84-uPAR cells.

10. References

1.   Kumar N, Sharma A, Khinchi M, Kuma C, Singh SPJAJoPR, Development. A Review on Different Types Of Cancer. 2017:1-8.

2.   Barnes L, Eveson J, Reichart P, Sidransky DJLI. World Health Organization classifications tumours. Pathology and genetics of head and neck tumours. 2005.

3.   Jerjes W, Upile T, Petrie A, Riskalla A, Hamdoon Z, Vourvachis M, et al. Clinicopathological parameters, recurrence, locoregional and distant metastasis in 115 T1-T2 oral squamous cell carcinoma patients. Head & neck oncology. 2010;2:9-.

4.   Leemans CR, Braakhuis BJ, Brakenhoff RHJNrc. The molecular biology of head and neck cancer. 2011;11(1):9.

5.   Cai X, Huang J. The Analysis of Oral Cancer on Pubmed from 2012 to 2016.

6.   Maturana-Ramírez A, Espinoza I, Reyes M, Aitken JP, Aguayo F, Hartel S, et al. Higher blood vessel density in comparison to the lymphatic vessels in oral squamous cell carcinoma. 2015;8(10):13677.

7.   Scully C, Felix DJBdj. Oral Medicine—Update for the dental practitioner Orofacial pain. 2006;200(2):75.

8.   Bolesina N, Femopase FL, de Blanc SAL, Morelatto RA, Olmos MA. Oral squamous cell carcinoma clinical aspects. Oral Cancer: InTech; 2012.

9.   Kamangar F, Dores GM, Anderson WF. Patterns of cancer incidence, mortality, and prevalence across five continents: defining priorities to reduce cancer disparities in different geographic regions of the world. J Clin Oncol. 2006;24(14):2137-50.

10.   Martinez C, Hernandez M, Martinez B, Adorno D. [Frequency of oral squamous cell carcinoma and oral epithelial dysplasia in oral and oropharyngeal mucosa in Chile]. Revista medica de Chile. 2016;144(2):169-74.

11.   Ogden GR. Alcohol and oral cancer. Alcohol (Fayetteville, NY). 2005;35(3):169-73.

12.   Petti S. Lifestyle risk factors for oral cancer. Oral Oncology. 2009;45(4):340-50.

13.   Bravi F, Bosetti C, Filomeno M, Levi F, Garavello W, Galimberti S, et al. Foods, nutrients and the risk of oral and pharyngeal cancer. 2013;109(11):2904.

14.   O'Sullivan B, Brierley J, Byrd D, Bosman F, Kehoe S, Kossary C, et al. The TNM classification of malignant tumours-towards common understanding and reasonable expectations. The Lancet Oncology. 2017;18(7):849-51.

15.   Bankfalvi A, Piffko J. Prognostic and predictive factors in oral cancer: the role of the invasive tumour front. Journal of oral pathology & medicine : official publication of the International Association of Oral Pathologists and the American Academy of Oral Pathology. 2000;29(7):291-8.

16.   Marsh D, Suchak K, Moutasim KA, Vallath S, Hopper C, Jerjes W, et al. Stromal features are predictive of disease mortality in oral cancer patients. The Journal of pathology. 2011;223(4):470-81.

17.   de Araujo RF, Jr., Barboza CA, Clebis NK, de Moura SA, Lopes Costa Ade L. Prognostic significance of the anatomical location and TNM clinical classification in oral squamous cell carcinoma. Medicina oral, patologia oral y cirugia bucal. 2008;13(6):E344-7.

18.   Slaughter DP, Southwick HW, Smejkal W. Field cancerization in oral stratified squamous epithelium; clinical implications of multicentric origin. Cancer. 1953;6(5):963-8.

19.   Day GL, Blot WJ, Shore RE, McLaughlin JK, Austin DF, Greenberg RS, et al. Second cancers following oral and pharyngeal cancers: role of tobacco and alcohol. Journal of the National Cancer Institute. 1994;86(2):131-7.

20.   Whiteside TL. The tumor microenvironment and its role in promoting tumor growth. Oncogene. 2008;27(45):5904-12.

21.   Schultz-Hector S, Haghayegh SJCr. β-Fibroblast growth factor expression in human and murine squamous cell carcinomas and its relationship to regional endothelial cell proliferation. 1993;53(6):1444-9.

22.   Joyce JA, Pollard JWJNrc. Microenvironmental regulation of metastasis. 2009;9(4):239.
23.   Maley F, Trimble RB, Tarentino AL, Plummer Jr THJAb. Characterization of glycoproteins and their associated oligosaccharides through the use of endoglycosidases. 1989;180(2):195-204.
24.   Alberts B, Bray D, Hopin K, Johnson A, Lewis J, Raff M, et al. Tissues and Cancer. Essential cell biology. 2004;2.
25.   Bussard KM, Mutkus L, Stumpf K, Gomez-Manzano C, Marini FCJBCR. Tumor-associated stromal cells as key contributors to the tumor microenvironment. 2016;18(1):84.
26.   Weinberg RA. The biology of cancer 2nd edition. Garland Science. Taylor & Francis Group; 2013.
27.   Armulik A, Abramsson A, Betsholtz C. Endothelial/pericyte interactions. Circulation research. 2005;97(6):512-23.
28.   Ferrara N, Hillan KJ, Novotny W. Bevacizumab (Avastin), a humanized anti-VEGF monoclonal antibody for cancer therapy. Biochemical and biophysical research communications. 2005;333(2):328-35.
29.   Folkman J. Angiogenesis in cancer, vascular, rheumatoid and other disease. Nature medicine. 1995;1(1):27-31.
30.   Wormann SM, Diakopoulos KN, Lesina M, Algul H. The immune network in pancreatic cancer development and progression. Oncogene. 2014;33(23):2956-67.
31.   Hanahan D, Coussens LM. Accessories to the crime: functions of cells recruited to the tumor microenvironment. Cancer cell. 2012;21(3):309-22.
32.   De Palma M, Coussens LM. Immune cells and inflammatory mediators as regulators of tumor angiogenesis. Angiogenesis: Springer; 2008. p. 225-37.
33.   Mantovani A, Allavena P, Sica A, Balkwill FJN. Cancer-related inflammation. 2008;454(7203):436.
34.   Ruffell B, DeNardo DG, Affara NI, Coussens LM. Lymphocytes in cancer development: polarization towards pro-tumor immunity. Cytokine & growth factor reviews. 2010;21(1):3-10.
35.   Shiao SL, Ganesan AP, Rugo HS, Coussens LMJG, development. Immune microenvironments in solid tumors: new targets for therapy. 2011;25(24):2559-72.
36.   Cook J, Hagemann TJCoip. Tumour-associated macrophages and cancer. 2013;13(4):595-601.
37.   Tarin D, Croft CB. Ultrastructural features of wound healing in mouse skin. Journal of anatomy. 1969;105(Pt 1):189-90.
38.   Magnussen S, Hadler-Olsen E, Latysheva N, Pirila E, Steigen SE, Hanes R, et al. Tumour microenvironments induce expression of urokinase plasminogen activator receptor (uPAR) and concomitant activation of gelatinolytic enzymes. 2014;9(8):e105929.
39.   Forsdahl S, Kiselev Y, Hogseth R, Mjelle JE, Mikkola IJPo. Pax6 regulates the expression of Dkk3 in murine and human cell lines, and altered responses to Wnt signaling are shown in FlpIn-3T3 cells stably expressing either the Pax6 or the Pax6 (5a) isoform. 2014;9(7):e102559.
40.   Todaro GJ, Green HJTJocb. Quantitative studies of the growth of mouse embryo cells in culture and their development into established lines. 1963;17(2):299-313.
41.   Vandooren J, Van den Steen PE, Opdenakker G. Biochemistry and molecular biology of gelatinase B or matrix metalloproteinase-9 (MMP-9): the next decade. Critical reviews in biochemistry and molecular biology. 2013;48(3):222-72.
42.   Räsänen K, Vaheri A. Activation of fibroblasts in cancer stroma. Experimental Cell Research. 2010;316(17):2713-22.
43.   Ronnov-Jessen L, Petersen OW, Bissell MJ. Cellular changes involved in conversion of normal to malignant breast: importance of the stromal reaction. Physiological reviews. 1996;76(1):69-125.
44.   Eyden B, Banerjee SS, Shenjere P, Fisher C. The myofibroblast and its tumours. Journal of clinical pathology. 2009;62(3):236-49.
45.   Mao Y, Keller ET, Garfield DH, Shen K, Wang J. Stromal cells in tumor microenvironment and breast cancer. Cancer metastasis reviews. 2013;32(1-2):303-15.

46.   Chomarat P, Banchereau J, Davoust J, Palucka AK. IL-6 switches the differentiation of monocytes from dendritic cells to macrophages. Nat Immunol. 2000;1(6):510-4.

47.   Bremnes RM, Donnem T, Al-Saad S, Al-Shibli K, Andersen S, Sirera R, et al. The role of tumor stroma in cancer progression and prognosis: emphasis on carcinoma-associated fibroblasts and non-small cell lung cancer. Journal of thoracic oncology : official publication of the International Association for the Study of Lung Cancer. 2011;6(1):209-17.

48.   Mitra AK, Zillhardt M, Hua Y, Tiwari P, Murmann AE, Peter ME, et al. MicroRNAs reprogram normal fibroblasts into cancer-associated fibroblasts in ovarian cancer. Cancer discovery. 2012;2(12):1100-8.

49.   Witsch E, Sela M, Yarden Y. Roles for growth factors in cancer progression. Physiology (Bethesda, Md). 2010;25(2):85-101.

50.   Bhowmick NA, Neilson EG, Moses HL. Stromal fibroblasts in cancer initiation and progression. Nature. 2004;432(7015):332-7.

51.   Song G, Ouyang G, Bao SJJoc, medicine m. The activation of Akt/PKB signaling pathway and cell survival. 2005;9(1):59-71.

52.   Kratchmarova I, Blagoev B, Haack-Sorensen M, Kassem M, Mann MJS. Mechanism of divergent growth factor effects in mesenchymal stem cell differentiation. 2005;308(5727):1472-7.

53.   Grotendorst GR, Smale G, Pencev D. Production of transforming growth factor beta by human peripheral blood monocytes and neutrophils. Journal of cellular physiology. 1989;140(2):396-402.

54.   Goulart IM, Mineo JR, Foss NT. Production of transforming growth factor-beta 1 (TGF-beta1) by blood monocytes from patients with different clinical forms of leprosy. Clinical and experimental immunology. 2000;122(3):330-4.

55.   Good M, Kolls JK, Empey KM. 130 - Neonatal Pulmonary Host Defense. In: Polin RA, Abman SH, Rowitch DH, Benitz WE, Fox WW, editors. Fetal and Neonatal Physiology (Fifth Edition): Elsevier; 2017. p. 1262-93.e12.

56.   Rifkin DBJJoBC. Latent transforming growth factor-β (TGF-β) binding proteins: orchestrators of TGF-β availability. 2005;280(9):7409-12.

57.   ten Dijke P, Arthur HM. Extracellular control of TGFbeta signalling in vascular development and disease. Nature reviews Molecular cell biology. 2007;8(11):857-69.

58.   Lu P, Takai K, Weaver VM, Werb Z. Extracellular matrix degradation and remodeling in development and disease. Cold Spring Harbor perspectives in biology. 2011;3(12):10.1101/cshperspect.a005058 a.

59.   Stetler-Stevenson WG, Aznavoorian S, Liotta LAJArocb. Tumor cell interactions with the extracellular matrix during invasion and metastasis. 1993;9(1):541-73.

60.   Barcellos-Hoff M, Dix TAJMe. Redox-mediated activation of latent transforming growth factor-beta 1. 1996;10(9):1077-83.

61.   Wipff P-J, Hinz BJEjocb. Integrins and the activation of latent transforming growth factor β1–an intimate relationship. 2008;87(8-9):601-15.

62.   Tang B, Vu M, Booker T, Santner SJ, Miller FR, Anver MR, et al. TGF-beta switches from tumor suppressor to prometastatic factor in a model of breast cancer progression. The Journal of clinical investigation. 2003;112(7):1116-24.

63.   Zhang YE. Non-Smad pathways in TGF-beta signaling. Cell research. 2009;19(1):128-39.

64.   Abbas T, Dutta AJNRC. p21 in cancer: intricate networks and multiple activities. 2009;9(6):400.

65.   Harper JW, Adami GR, Wei N, Keyomarsi K, Elledge SJJC. The p21 Cdk-interacting protein Cip1 is a potent inhibitor of G1 cyclin-dependent kinases. 1993;75(4):805-16.

66.   Katz LH, Li Y, Chen J-S, Muñoz NM, Majumdar A, Chen J, et al. Targeting TGF-β signaling in cancer. Expert opinion on therapeutic targets. 2013;17(7):743-60.

67.   Hartsough MT, Mulder KMJJoBC. Transforming growth factor β activation of p44mapk in proliferating cultures of epithelial cells. 1995;270(13):7117-24.

68.   Nieto MA, Huang RY, Jackson RA, Thiery JP. EMT: 2016. Cell. 2016;166(1):21-45.

69.   Lee JM, Dedhar S, Kalluri R, Thompson EW. The epithelial-mesenchymal transition: new insights in signaling, development, and disease. The Journal of cell biology. 2006;172(7):973-81.

70.   Shin I, Bakin AV, Rodeck U, Brunet A, Arteaga CLJMbotc. Transforming growth factor β enhances epithelial cell survival via Akt-dependent regulation of FKHRL1. 2001;12(11):3328-39.

71.   Chen R-H, Su Y-H, Chuang RL, Chang T-YJO. Suppression of transforming growth factor-β-induced apoptosis through a phosphatidylinositol 3-kinase/Akt-dependent pathway. 1998;17(15):1959.

72.   Song K, Wang H, Krebs TL, Danielpour DJTEj. Novel roles of Akt and mTOR in suppressing TGF-β/ALK5-mediated Smad3 activation. 2006;25(1):58-69.

73.   Page-McCaw A, Ewald AJ, Werb Z. Matrix metalloproteinases and the regulation of tissue remodelling. Nature reviews Molecular cell biology. 2007;8(3):221-33.

74.   Conlon GA, Murray GI. Recent advances in understanding the roles of matrix metalloproteinases in tumour invasion and metastasis. The Journal of pathology. 2019;247(5):629-40.

75.   Mittal R, Patel AP, Debs LH, Nguyen D, Patel K, Grati M, et al. Intricate Functions of Matrix Metalloproteinases in Physiological and Pathological Conditions. Journal of cellular physiology. 2016;231(12):2599-621.

76.   Snoek-van Beurden PA, Von den Hoff JW. Zymographic techniques for the analysis of matrix metalloproteinases and their inhibitors. BioTechniques. 2005;38(1):73-83.

77.   Gialeli C, Theocharis AD, Karamanos NK. Roles of matrix metalloproteinases in cancer progression and their pharmacological targeting. The FEBS journal. 2011;278(1):16-27.

78.   Corcoran ML, Hewitt RE, Kleiner DE, Jr., Stetler-Stevenson WG. MMP-2: expression, activation and inhibition. Enzyme & protein. 1996;49(1-3):7-19.

79.   Theret N, Lehti K, Musso O, Clement B. MMP2 activation by collagen I and concanavalin A in cultured human hepatic stellate cells. Hepatology (Baltimore, Md). 1999;30(2):462-8.

80.   Mook OR, Frederiks WM, Van Noorden CJ. The role of gelatinases in colorectal cancer progression and metastasis. Biochimica et biophysica acta. 2004;1705(2):69-89.

81.   Van den Steen PE, Dubois B, Nelissen I, Rudd PM, Dwek RA, Opdenakker G. Biochemistry and molecular biology of gelatinase B or matrix metalloproteinase-9 (MMP-9). Critical reviews in biochemistry and molecular biology. 2002;37(6):375-536.

82.   Delclaux C, Delacourt C, D'Ortho MP, Boyer V, Lafuma C, Harf A. Role of gelatinase B and elastase in human polymorphonuclear neutrophil migration across basement membrane. American journal of respiratory cell and molecular biology. 1996;14(3):288-95.

83.   Dubois B, Starckx S, Pagenstecher A, Oord J, Arnold B, Opdenakker G. Gelatinase B deficiency protects against endotoxin shock. European journal of immunology. 2002;32(8):2163-71.

84.   Heissig B, Hattori K, Dias S, Friedrich M, Ferris B, Hackett NR, et al. Recruitment of stem and progenitor cells from the bone marrow niche requires MMP-9 mediated release of kit-ligand. Cell. 2002;109(5):625-37.

85.   Morini M, Mottolese M, Ferrari N, Ghiorzo F, Buglioni S, Mortarini R, et al. The alpha 3 beta 1 integrin is associated with mammary carcinoma cell metastasis, invasion, and gelatinase B (MMP-9) activity. International journal of cancer. 2000;87(3):336-42.

86.   Zucker S, Lysik RM, DiMassimo BI, Zarrabi HM, Moll UM, Grimson R, et al. Plasma assay of gelatinase B: tissue inhibitor of metalloproteinase complexes in cancer. Cancer. 1995;76(4):700-8.

87.   Aisina RB, Mukhametova LI. [Structure and functions of plasminogen/plasmin system]. Bioorganicheskaia khimiia. 2014;40(6):642-57.

88.   Mahmood N, Mihalcioiu C, Rabbani SA. Multifaceted Role of the Urokinase-Type Plasminogen Activator (uPA) and Its Receptor (uPAR): Diagnostic, Prognostic, and Therapeutic Applications. Frontiers in oncology. 2018;8:24.

89.   Andreasen PA, Egelund R, Petersen HH. The plasminogen activation system in tumor growth, invasion, and metastasis. Cellular and molecular life sciences : CMLS. 2000;57(1):25-40.

90.   Leurer C, Rabbani SA. Plasminogen activator system—diagnostic, prognostic and therapeutic implications in breast cancer. A Concise Review of Molecular Pathology of Breast Cancer: IntechOpen; 2015.

91.   Kugaevskaya EV, Gureeva TA, Timoshenko OS, Solovyeva NI. [The urokinase-type plasminogen activator system and its role in tumor progression]. Biomeditsinskaia khimiia. 2018;64(6):472-86.

92.   Andreasen PA, Kjoller L, Christensen L, Duffy MJ. The urokinase-type plasminogen activator system in cancer metastasis: a review. International journal of cancer. 1997;72(1):1-22.

93.   Irigoyen J, Munoz-Canoves P, Montero L, Koziczak M, Nagamine YJC, CMLS MLS. The plasminogen activator system: biology and regulation. 1999;56(1-2):104-32.

94.   Dano K, Andreasen PA, Grondahl-Hansen J, Kristensen P, Nielsen LS, Skriver L. Plasminogen activators, tissue degradation, and cancer. Advances in cancer research. 1985;44:139-266.

95.   Collen DJT, haemostasis. The plasminogen (fibrinolytic) system. 1999;82(08):259-70.

96.   Andreasen P, Egelund R, Petersen HJC, CMLS MLS. The plasminogen activation system in tumor growth, invasion, and metastasis. 2000;57(1):25-40.

97.   Ellis V, Scully MF, Kakkar VV. Plasminogen activation initiated by single-chain urokinase-type plasminogen activator. Potentiation by U937 monocytes. The Journal of biological chemistry. 1989;264(4):2185-8.

98.   Ellis V, Whawell SA, Werner F, Deadman JJ. Assembly of urokinase receptor-mediated plasminogen activation complexes involves direct, non-active-site interactions between urokinase and plasminogen. Biochemistry. 1999;38(2):651-9.

99.   Dass K, Ahmad A, Azmi AS, Sarkar SH, Sarkar FH. Evolving role of uPA/uPAR system in human cancers. Cancer treatment reviews. 2008;34(2):122-36.

100.   Wu G, Quek AJ, Caradoc-Davies TT, Ekkel SM, Mazzitelli B, Whisstock JC, et al. Structural studies of plasmin inhibition. Biochemical Society transactions. 2019.

101.   Duffy MJ, O'Grady P. Plasminogen activator and cancer. European Journal of Cancer and Clinical Oncology. 1984;20(5):577-82.

102.   Zhang Z, Pan J, Li L, Wang Z, Xiao W, Li NJJoOP, et al. Survey of risk factors contributed to lymphatic metastasis in patients with oral tongue cancer by immunohistochemistry. 2011;40(2):127-34.

103.   Kumari S, Malla R. New Insight on the Role of Plasminogen Receptor in Cancer Progression. Cancer growth and metastasis. 2015;8:35-42.

104.   Al-Horani RA. Serpin regulation of fibrinolytic system: implications for therapeutic applications in cardiovascular diseases. Cardiovascular & hematological agents in medicinal chemistry. 2014;12(2):91-125.

105.   Iishi H, Tatsuta M, Baba M, Yano H, Uehara H, Nakaizumi A. Suppression by amiloride of bombesin-enhanced peritoneal metastasis of intestinal adenocarcinomas induced by azoxymethane. International journal of cancer. 1995;63(5):716-9.

106.   WyganoWSka-ŚWiątkoWSka M, Jankun JJIjoo. Plasminogen activation system in oral cancer: Relevance in prognosis and therapy. 2015;47(1):16-24.

107.   Beaufort N, Leduc D, Rousselle JC, Namane A, Chignard M, Pidard D. Plasmin cleaves the juxtamembrane domain and releases truncated species of the urokinase receptor (CD87) from human bronchial epithelial cells. FEBS letters. 2004;574(1-3):89-94.

108.   Carriero MV, Franco P, Del Vecchio S, Massa O, Botti G, D'Aiuto G, et al. Tissue distribution of soluble and receptor-bound urokinase in human breast cancer using a panel of monoclonal antibodies. Cancer research. 1994;54(20):5445-54.

109.   Jo M, Thomas KS, O'Donnell DM, Gonias SL. Epidermal growth factor receptor-dependent and -independent cell-signaling pathways originating from the urokinase receptor. The Journal of biological chemistry. 2003;278(3):1642-6.

110.   Kjoller L, Hall A. Rac mediates cytoskeletal rearrangements and increased cell motility induced by urokinase-type plasminogen activator receptor binding to vitronectin. The Journal of cell biology. 2001;152(6):1145-57.

111.   Ossowski L, Aguirre-Ghiso JA. Urokinase receptor and integrin partnership: coordination of signaling for cell adhesion, migration and growth. Current opinion in cell biology. 2000;12(5):613-20.

112.   Zhang G, Cai X, Lopez-Guisa JM, Collins SJ, Eddy AA. Mitogenic signaling of urokinase receptor-deficient kidney fibroblasts: actions of an alternative urokinase receptor and LDL receptor-related protein. Journal of the American Society of Nephrology : JASN. 2004;15(8):2090-102.

113.   Koolwijk P, Sidenius N, Peters E, Sier CF, Hanemaaijer R, Blasi F, et al. Proteolysis of the urokinase-type plasminogen activator receptor by metalloproteinase-12: implication for angiogenesis in fibrin matrices. Blood. 2001;97(10):3123-31.

114.   Hoyer-Hansen G, Ronne E, Solberg H, Behrendt N, Ploug M, Lund LR, et al. Urokinase plasminogen activator cleaves its cell surface receptor releasing the ligand-binding domain. The Journal of biological chemistry. 1992;267(25):18224-9.

115.   Ragno P, Montuori N, Covelli B, Hoyer-Hansen G, Rossi GJCr. Differential expression of a truncated form of the urokinase-type plasminogen-activator receptor in normal and tumor thyroid cells. 1998;58(6):1315-9.

116.   Wilhelm OG, Wilhelm S, Escott GM, Lutz V, Magdolen V, Schmitt M, et al. Cellular glycosylphosphatidylinositol-specific phospholipase D regulates urokinase receptor shedding and cell surface expression. Journal of cellular physiology. 1999;180(2):225-35.

117.   Blasi F, Carmeliet PJNrMcb. uPAR: a versatile signalling orchestrator. 2002;3(12):932.

118.   Bianchi E, Cohen RL, Thor AT, Todd RF, 3rd, Mizukami IF, Lawrence DA, et al. The urokinase receptor is expressed in invasive breast cancer but not in normal breast tissue. Cancer research. 1994;54(4):861-6.

119.   Jo M, Takimoto S, Montel V, Gonias SL. The urokinase receptor promotes cancer metastasis independently of urokinase-type plasminogen activator in mice. The American journal of pathology. 2009;175(1):190-200.

120.   Estreicher A, Muhlhauser J, Carpentier JL, Orci L, Vassalli JD. The receptor for urokinase type plasminogen activator polarizes expression of the protease to the leading edge of migrating monocytes and promotes degradation of enzyme inhibitor complexes. The Journal of cell biology. 1990;111(2):783-92.

121.   Wei Y, Lukashev M, Simon DI, Bodary SC, Rosenberg S, Doyle MV, et al. Regulation of integrin function by the urokinase receptor. Science (New York, NY). 1996;273(5281):1551-5.

122.   Vaughan MB, Howard EW, Tomasek JJ. Transforming growth factor-beta1 promotes the morphological and functional differentiation of the myofibroblast. Exp Cell Res. 2000;257(1):180-9.

123.   Hinz B, Gabbiani G. Mechanisms of force generation and transmission by myofibroblasts. Curr Opin Biotechnol. 2003;14(5):538-46.

124.   Bernstein AM, Greenberg RS, Taliana L, Masur SK. Urokinase anchors uPAR to the actin cytoskeleton. Investigative ophthalmology & visual science. 2004;45(9):2967-77.

125.   Arora S, Kaur J, Sharma C, Mathur M, Bahadur S, Shukla NK, et al. Stromelysin 3, Ets-1, and vascular endothelial growth factor expression in oral precancerous and cancerous lesions: correlation with microvessel density, progression, and prognosis. Clinical cancer research : an official journal of the American Association for Cancer Research. 2005;11(6):2272-84.

126.   Shiraki M, Odajima T, Ikeda T, Sasaki A, Satoh M, Yamaguchi A, et al. Combined expression of p53, cyclin D1 and epidermal growth factor receptor improves estimation of prognosis in curatively resected

oral cancer. Modern pathology : an official journal of the United States and Canadian Academy of Pathology, Inc. 2005;18(11):1482-9.

127.   Hadler-Olsen E, Wirsing AMJBjoc. Tissue-infiltrating immune cells as prognostic markers in oral squamous cell carcinoma: a systematic review and meta-analysis. 2019:1.

128.   Kartha VK, Stawski L, Han R, Haines P, Gallagher G, Noonan V, et al. PDGFRbeta Is a Novel Marker of Stromal Activation in Oral Squamous Cell Carcinomas. PloS one. 2016;11(4):e0154645.

129.   Kumcu E, Unverdi H, Kaymaz E, Oral O, Turkbey D, Hucmenoglu S. Stromal podoplanin expression and its clinicopathological role in breast carcinoma. The Malaysian journal of pathology. 2018;40(2):137-42.

130.   Chuaysri C, Thuwajit P, Paupairoj A, Chau-In S, Suthiphongchai T, Thuwajit C. Alpha-smooth muscle actin-positive fibroblasts promote biliary cell proliferation and correlate with poor survival in cholangiocarcinoma. Oncology reports. 2009;21(4):957-69.

131.   Paulsson J, Micke P. Prognostic relevance of cancer-associated fibroblasts in human cancer. Seminars in cancer biology. 2014;25:61-8.

132.   Erdogan B, Webb DJ. Cancer-associated fibroblasts modulate growth factor signaling and extracellular matrix remodeling to regulate tumor metastasis. Biochemical Society transactions. 2017;45(1):229-36.

133.   Magnussen SN, Hadler-Olsen E, Costea DE, Berg E, Jacobsen CC, Mortensen B, et al. Cleavage of the urokinase receptor (uPAR) on oral cancer cells: regulation by transforming growth factor–β1 (TGF-β1) and potential effects on migration and invasion. 2017;17(1):350.

134.   Lou E, Kellman R, Hutchison R, Shillitoe EJOd. Clinical and pathological features of the murine AT-84 orthotopic model of oral cancer. 2003;9(6):305-12.

135.   Wetting HL, Hadler-Olsen E, Magnussen S, Rikardsen O, Steigen SE, Sundkvist E, et al. S100A4 expression in xenograft tumors of human carcinoma cell lines is induced by the tumor microenvironment. 2011;178(5):2389-96.

136.   Lowry OH, Rosebrough NJ, Farr AL, Randall RJJJobc. Protein measurement with the Folin phenol reagent. 1951;193:265-75.

137.   Peterson GLJAb. Review of the Folin phenol protein quantitation method of Lowry, Rosebrough, Farr and Randall. 1979;100(2):201-20.

138.   Vandooren J, Geurts N, Martens E, Van den Steen PE, Opdenakker GJNm. Zymography methods for visualizing hydrolytic enzymes. 2013;10(3):211.

139.   Ramos-Vara J, Miller MJVp. When tissue antigens and antibodies get along: revisiting the technical aspects of immunohistochemistry—the red, brown, and blue technique. 2014;51(1):42-87.

140.   Coons AH, Creech HJ, Jones RNJPotSfEB, Medicine. Immunological properties of an antibody containing a fluorescent group. 1941;47(2):200-2.

141.   He Y, Chen Z-y, Zhu J, Xiong Y, Li K, Dong J-h, et al. Interaction between cancer cells and stromal fibroblasts is required for activation of the uPAR-uPA-MMP-2 cascade in pancreatic cancer metastasis. 2007;13(11):3115-24.

142.   Noh H, Hong S, Huang S. Role of urokinase receptor in tumor progression and development. Theranostics. 2013;3(7):487-95.

143.   Di Mauro C, Pesapane A, Formisano L, Rosa R, D'Amato V, Ciciola P, et al. Urokinase-type plasminogen activator receptor (uPAR) expression enhances invasion and metastasis in RAS mutated tumors. 2017;7(1):9388.

144.   Simone TM, Higgins SP, Archambeault J, Higgins CE, Ginnan RG, Singer H, et al. A small molecule PAI-1 functional inhibitor attenuates neointimal hyperplasia and vascular smooth muscle cell survival by promoting PAI-1 cleavage. Cellular signalling. 2015;27(5):923-33.

145.   Östman AJC, reviews gf. PDGF receptors-mediators of autocrine tumor growth and regulators of tumor vasculature and stroma. 2004;15(4):275-86.

146.   Matsushima T, Kobuna I, Sugimura TJN. In vivo interaction of 4-nitroquinoline-l-oxide and its derivatives with DNA. 1967;216(5114):508.

147.   Freshney RI. Culture of animal cells: Wiley Online Library; 2005.

148.   Freshney RIJCocfte. Basic principles of cell culture. 2006;11-4.

149.   Arora MJMm. Cell culture media: a review. 2013;3(175):24.

150.   Strehl R, Schumacher K, de Vries U, Minuth WWJTe. Proliferating cells versus differentiated cells in tissue engineering. 2002;8(1):37-42.

151.   Chua K, Aminuddin B, Fuzina N, Ruszymah BJECM. Insulin-transferrin-selenium prevent human chondrocyte dedifferentiation and promote the formation of high quality tissue engineered human hyaline cartilage. 2005;9(9):58-67.

152.   Verwoerd-Verhoef HJP, surgery r. In vitro redifferentiation of culture-expanded rabbit and human auricular chondrocytes for cartilage reconstruction. 2001;107(2):433-40.

153.   Zhang L, Song H, Zhao XJIjocb. Optimum combination of insulin-transferrin-selenium and fetal bovine serum for culture of rabbit articular chondrocytes in three-dimensional alginate scaffolds. 2009;2009.

154.   Herrler A, Krusche CA, Beier HM. Insulin and insulin-like growth factor-I promote rabbit blastocyst development and prevent apoptosis. Biology of reproduction. 1998;59(6):1302-10.

155.   Merlo GR, Graus-Porta D, Cella N, Marte BM, Taverna D, Hynes NE. Growth, differentiation and survival of HC11 mammary epithelial cells: diverse effects of receptor tyrosine kinase-activating peptide growth factors. European journal of cell biology. 1996;70(2):97-105.

156.   Bremnes RM, Dønnem T, Al-Saad S, Al-Shibli K, Andersen S, Sirera R, et al. The Role of Tumor Stroma in Cancer Progression and Prognosis: Emphasis on Carcinoma-Associated Fibroblasts and Non-small Cell Lung Cancer. Journal of Thoracic Oncology. 2011;6(1):209-17.

157.   Kalluri R, Zeisberg MJNRC. Fibroblasts in cancer. 2006;6(5):392.

158.   Kasabova M, Joulin-Giet A, Lecaille F, Gilmore BF, Marchand-Adam S, Saidi A, et al. Regulation of TGF-beta1-driven differentiation of human lung fibroblasts: emerging roles of cathepsin B and cystatin C. The Journal of biological chemistry. 2014;289(23):16239-51.

159.   Chen X, Thibeault SL. Response of fibroblasts to transforming growth factor-β1 on two-dimensional and in three-dimensional hyaluronan hydrogels. Tissue engineering Part A. 2012;18(23-24):2528-38.

160.   Siren V, Salmenpera P, Kankuri E, Bizik J, Sorsa T, Tervahartiala T, et al. Cell-cell contact activation of fibroblasts increases the expression of matrix metalloproteinases. Annals of medicine. 2006;38(3):212-20.

161.   Kayamori K, Katsube K, Sakamoto K, Ohyama Y, Hirai H, Yukimori A, et al. NOTCH3 Is Induced in Cancer-Associated Fibroblasts and Promotes Angiogenesis in Oral Squamous Cell Carcinoma. PloS one. 2016;11(4):e0154112.

162.   Lin NN, Wang P, Zhao D, Zhang FJ, Yang K, Chen R. Significance of oral cancer-associated fibroblasts in angiogenesis, lymphangiogenesis, and tumor invasion in oral squamous cell carcinoma. Journal of oral pathology & medicine : official publication of the International Association of Oral Pathologists and the American Academy of Oral Pathology. 2017;46(1):21-30.

163.   de-Assis EM, Pimenta LG, Costa-e-Silva E, Souza PE, Horta MC. Stromal myofibroblasts in oral leukoplakia and oral squamous cell carcinoma. Medicina oral, patologia oral y cirugia bucal. 2012;17(5):e733-8.

164.   Dourado RC, Porto LPA, Leitao A, Cerqueira PSG, Dos Santos JN, Ramalho LMP, et al. Immunohistochemical Characterization of Cancer-associated Fibroblasts in Oral Squamous Cell Carcinoma. Applied immunohistochemistry & molecular morphology : AIMM. 2018;26(9):640-7.

165.   Høyer-Hansen G, Rønne E, Solberg H, Behrendt N, Ploug M, Lund L, et al. Urokinase plasminogen activator cleaves its cell surface receptor releasing the ligand-binding domain. 1992;267(25):18224-9.

166.   Hoyer-Hansen G, Pessara U, Holm A, Pass J, Weidle U, Dano K, et al. Urokinase-catalysed cleavage of the urokinase receptor requires an intact glycolipid anchor. The Biochemical journal. 2001;358(Pt 3):673-9.

167.   Hoyer-Hansen G, Ploug M, Behrendt N, Ronne E, Dano K. Cell-surface acceleration of urokinase-catalyzed receptor cleavage. European journal of biochemistry. 1997;243(1-2):21-6.

168.   McCawley LJ, Matrisian LMJMmt. Matrix metalloproteinases: multifunctional contributors to tumor progression. 2000;6(4):149-56.

169.   Giannelli G, Falk-Marzillier J, Schiraldi O, Stetler-Stevenson WG, Quaranta VJS. Induction of cell migration by matrix metalloprotease-2 cleavage of laminin-5. 1997;277(5323):225-8.

170.   Czekay R-P, Wilkins-Port CE, Higgins SP, Freytag J, Overstreet JM, Klein RM, et al. PAI-1: an integrator of cell signaling and migration. 2011;2011.

171.   Kutz SM, Hordines J, McKeown-Longo PJ, Higgins PJJJoCS. TGF-β1-induced PAI-1 gene expression requires MEK activity and cell-to-substrate adhesion. 2001;114(21):3905-14.

172.   Reilly C, McFall RJJoBC. Platelet-derived growth factor and transforming growth factor-beta regulate plasminogen activator inhibitor-1 synthesis in vascular smooth muscle cells. 1991;266(15):9419-27.

173.   Degryse B, Neels JG, Czekay RP, Aertgeerts K, Kamikubo Y, Loskutoff DJ. The low density lipoprotein receptor-related protein is a motogenic receptor for plasminogen activator inhibitor-1. The Journal of biological chemistry. 2004;279(21):22595-604.

174.   Herz J, Hamann U, Rogne S, Myklebost O, Gausepohl H, Stanley KKJTEj. Surface location and high affinity for calcium of a 500-kd liver membrane protein closely related to the LDL-receptor suggest a physiological role as lipoprotein receptor. 1988;7(13):4119-27.

175.   Lillis A, Mikhailenko I, Strickland DJJoT, Haemostasis. Beyond endocytosis: LRP function in cell migration, proliferation and vascular permeability. 2005;3(8):1884-93.

176.   Herz J, Strickland DKJTJoci. LRP: a multifunctional scavenger and signaling receptor. 2001;108(6):779-84.

177.   Cubellis MV, Wun T-C, Blasi FJTEJ. Receptor-mediated internalization and degradation of urokinase is caused by its specific inhibitor PAI-1. 1990;9(4):1079-85.

178.   Mauro CD, Pesapane A, Formisano L, Rosa R, D'Amato V, Ciciola P, et al. Urokinase-type plasminogen activator receptor (uPAR) expression enhances invasion and metastasis in RAS mutated tumors. Sci Rep. 2017;7(1):9388.

179.   Fazioli F, Resnati M, Sidenius N, Higashimoto Y, Appella E, Blasi FJTEJ. A urokinase-sensitive region of the human urokinase receptor is responsible for its chemotactic activity. 1997;16(24):7279-86.

180.   Degryse B, Resnati M, Rabbani SA, Villa A, Fazioli F, Blasi FJB. Src-dependence and pertussis-toxin sensitivity of urokinase receptor-dependent chemotaxis and cytoskeleton reorganization in rat smooth muscle cells. 1999;94(2):649-62.

181.   Rossi FW, Prevete N, Rivellese F, Napolitano F, Montuori N, Postiglione L, et al. The Urokinase/Urokinase Receptor System in Mast Cells: Effects of its Functional Interaction with fMLF Receptors. Translational medicine @ UniSa. 2016;15:34-41.

182.   Tarui T, Mazar AP, Cines DB, Takada YJJoBC. Urokinase-type plasminogen activator receptor (CD87) is a ligand for integrins and mediates cell-cell interaction. 2001;276(6):3983-90.

183.   Nishimura K, Matsumiya K, Miura H, Tsujimura A, Nonomura N, Matsumoto K, et al. Effects of hepatocyte growth factor on urokinase-type plasminogen activator (uPA) and uPA receptor in DU145 prostate cancer cells. International journal of andrology. 2003;26(3):175-9.

184.   Selleri C, Montuori N, Ricci P, Visconte V, Baiano A, Carriero MV, et al. In vivo activity of the cleaved form of soluble urokinase receptor: a new hematopoietic stem/progenitor cell mobilizer. Cancer research. 2006;66(22):10885-90.

185.   Garcia CM, Kwon GP, Beebe DC. alpha-Smooth muscle actin is constitutively expressed in the lens epithelial cells of several species. Experimental eye research. 2006;83(4):999-1001.

186.   Direkze NC, Hodivala-Dilke K, Jeffery R, Hunt T, Poulsom R, Oukrif D, et al. Bone marrow contribution to tumor-associated myofibroblasts and fibroblasts. 2004;64(23):8492-5.

187.   Ludin A, Itkin T, Gur-Cohen S, Mildner A, Shezen E, Golan K, et al. Monocytes-macrophages that express α-smooth muscle actin preserve primitive hematopoietic cells in the bone marrow. Nature Immunology. 2012;13:1072.

188.   Mazar APJCcr. Urokinase plasminogen activator receptor choreographs multiple ligand interactions: implications for tumor progression and therapy. 2008;14(18):5649-55.

189.   Lester RD, Jo M, Montel V, Takimoto S, Gonias SLJTJocb. uPAR induces epithelial–mesenchymal transition in hypoxic breast cancer cells. 2007;178(3):425-36.

11. Appendix/Supplementary Data

Appendix 11.1. The figure of Flp-In 3T3 cells showing their appearance at 72hr. (**a**) in DMEM and (**b**) RPMI media with different supplement. **1** -SFM, **2** -SFM + ITS, **3** -0.1% FBS, **4** -0.1% FBS plus ITS, **5** -0.5% FBS, **6** -0.5% FBS plus ITS, **7** -2% FBS, **8** -2% FBS plus ITS, **9** –Triton X-100 and **10** -10% FBS.
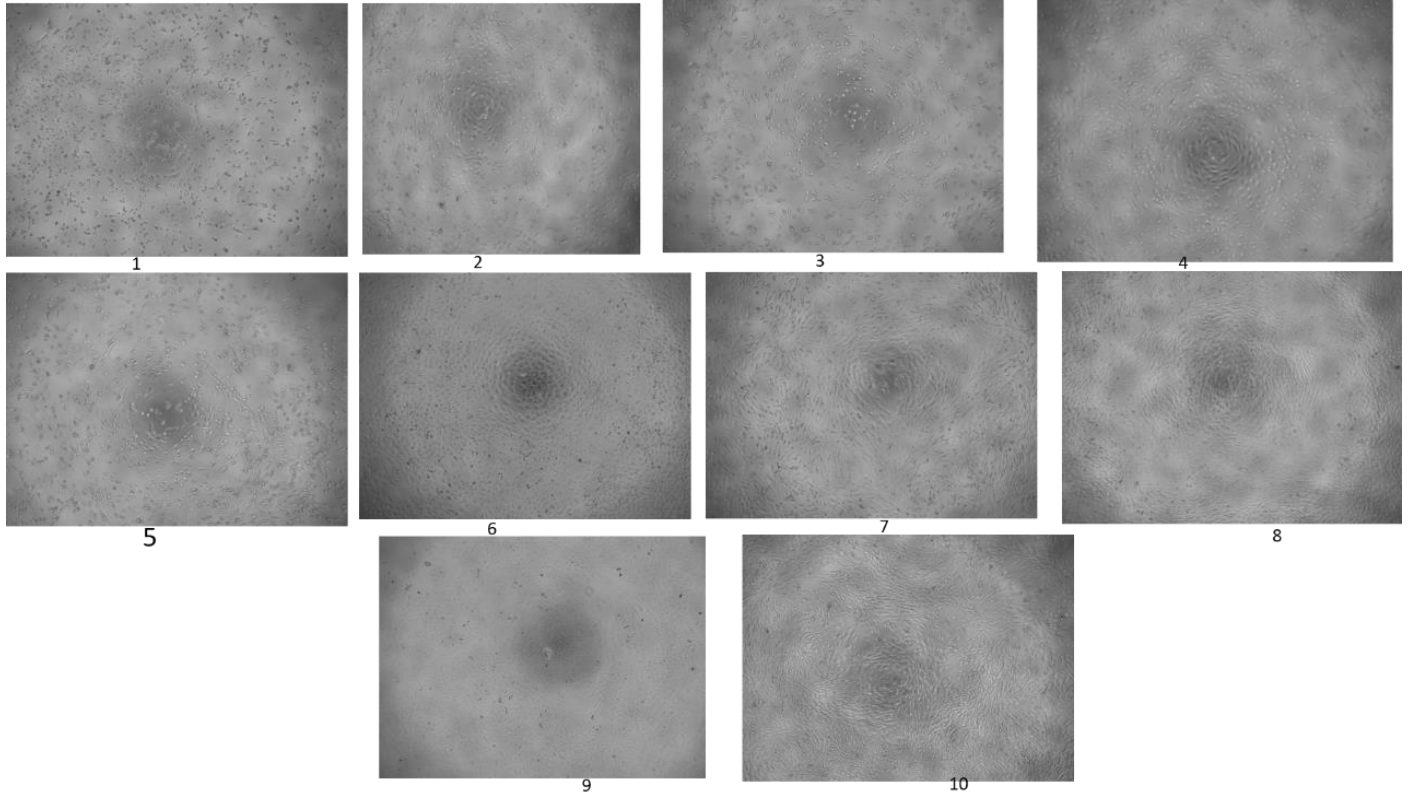

DMEM 72
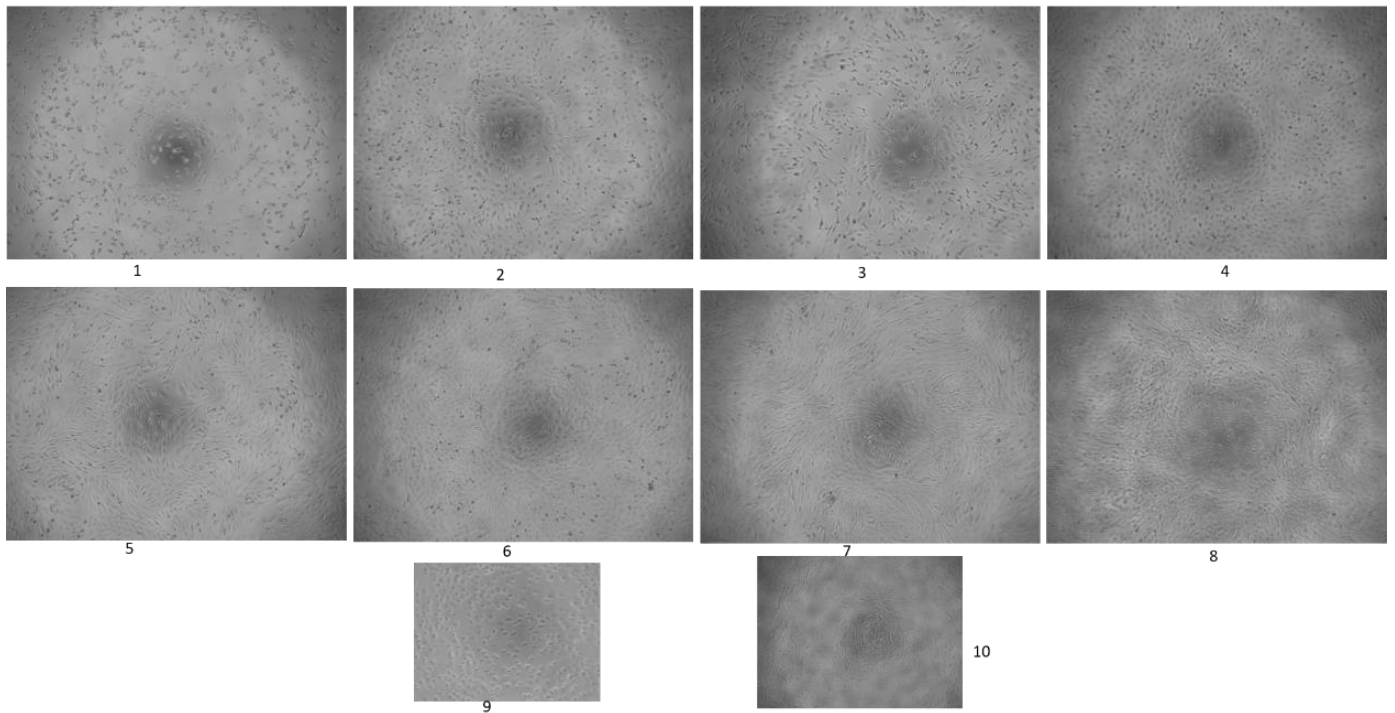
a.

RPMI 72hr

b.

Appendix 11. 2. **Tables showing the α- SMA expression quantification from western blot results using ImageJ. a**. shows 24, **b**. 48 and **c.** 72 hours expression of α-SMA. The expression of α-SMA was obtained by normalizing the loading control by considering the highest value of α-tubulin as standard (21302.67). The loading control of each sample was normalized by taking ratio of standard to its α-tubulin (standard/α-Tubulin). The α-SMA expression of each sample was then calculated by multiplying its value with its normalized loading control.

a

		24hr		aSMA	a-Tubulin		expression	Average	SD	T-test
1	without TGF	24hr		9750.388	18411.31	1.157043	11281.62	14737.43	3023.477	0.142627
2	without TGF	24hr		15356.97	19363.65	1.100137	16894.77			
3	without TGF	24hr		16035.92	21302.67	1	16035.92			
1	with TGF	24hr		22014.47	20234.67	1.052781	23176.41	19843.27	3734.779	
2	with TGF	24hr		19344.24	20056.11	1.062154	20546.56			
3	with TGF	24hr		14013.39	18885.65	1.127982	15806.85			
	without TGF	72hr		7562.903	18682.89	1.140223	8623.399			
	with TGF	72hr		9670.673	16058.92	1.326532	12828.46			

b.

		A-SMA	A-Tubulin	normalization of a-Tubulin	Expression	Average	SD	T-test
Without TGF-β	48hr	6488.196	21061.82	1.362882	8842.647	13387	4350	0.0278425
Without TGF-β	48hr	13662.15	22394.95	1.281753	17511.49			
Without TGF-β	48hr	10749.97	22348.43	1.284421	13807.49			
With TGF-β	48hr	17155.1	20929.33	1.37151	23528.39	22466	1660	
With TGF-β	48hr	16724.39	20588.65	1.394204	23317.21			
With TGF-β	48hr	19542.34	27292.37	1.051751	20553.68			
Without TGF-β	72hr+24	1596.548	19403.48	1.479363	2361.874			
With TGF-β	72hr+24	23274.77	28704.79	1	23274.77			

c.

Treatment group	Time of activation	α-SMA	α-Tubulin	Normalization	Expression	Average	SD	T-test
without TGF	72hr	11478.39	19080.82	1.090893	12521.69	11159.45	1237.988	0.000762
without TGF	72hr	10103.05	20815.14	1	10103.05			
without TGF	72hr	8502.095	16305.36	1.276583	10853.63			
with TGF	72hr	15575.58	16175.97	1.286794	20042.57	20206.69	1136.8	
with TGF	72hr	17384.22	18885.09	1.1022	19160.88			
with TGF	72hr	19839.39	19282.19	1.079501	21416.64			
without TGF	48hr	12449.36	16774.72	1.240863	15447.95			
with TGF	48hr	17318.12	19786.72	1.051975	18218.22			

Appendix 11.3. Quantification data of α-SMA expression in CMs treated Flp-In 3T3 cells.

Medium	CM2 EV	CM2 uPAR
14208.06	3802.695	4301.642
17617.86	4834.196	4161.342
10772.13	3382.096	2165.574
11424.77	4085.217	5908.824
12223.12	2950.170	2452.003
	5392.359	2574.197

**Appendix 11.4. Quantification data of uPAR ratio (DI-III/DIIDIII) in CM-Flp⁺ and CM-Flp±
treated AT84-uPAR cells.**

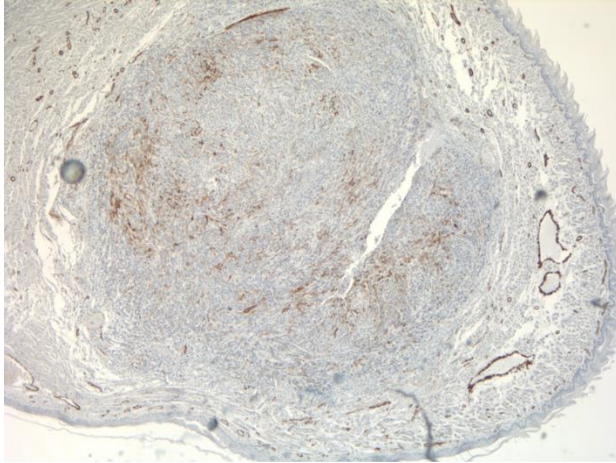| + TGFβ1	÷TGFβ1
1.827660	0.443947
1.015930	0.415424
1.187020	0.415333
1.291007	0.756040
1.499135	0.664120
2.083610	0.763780

Appendix 11.5. AT84 cells construct and uPAR expression. a. Image depicts the construct of AT84 cells, **b**. uPAR expression of cells (pre-injection to mouse tongue) and **c**. uPAR score *in vivo* in tongue tumor sections (SI= average staining index)**.** EV1=**EV3**, EV2=**EV4**, uPAR1=**uPAR2-2** and uPAR2=**uPAR2-3**. Taken and modified from (38).
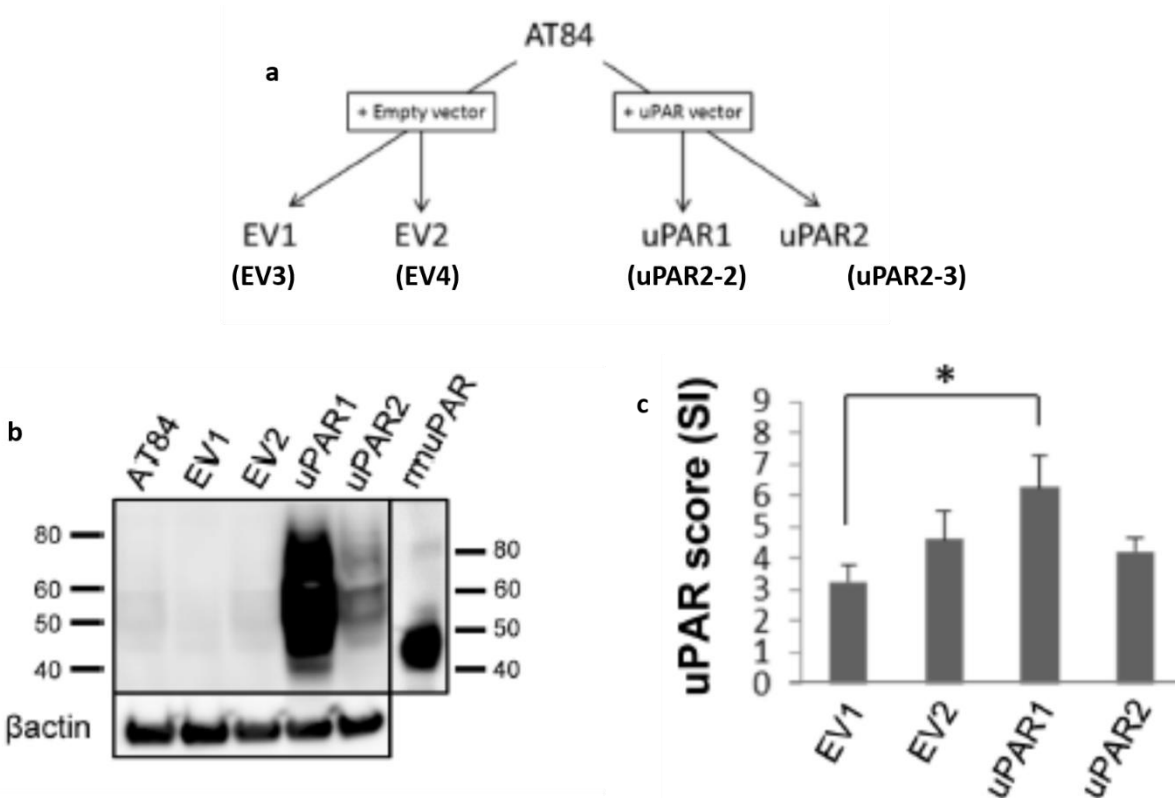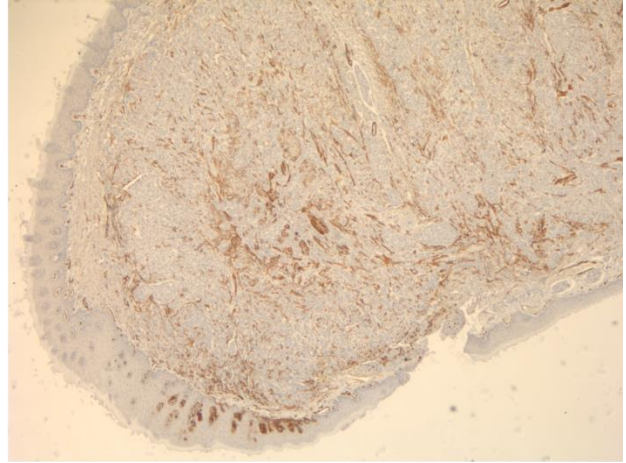
Appendix 11. 6. Quantification percentage data on CAF score using Immunoratio in each tongue tumor sections included in the analysis.

uPAR2-2	uPAR2-3	EV3	EV4
33.9	23.3	25.8	19.2
34.1	7.5	20.4	31.3
26.2	20.4	33.7	18.4
29.8	17.4	24.8	22.9
25.6	13.4	29.4	17.9
27.9	20.6	30.8	
24.6	26.8	36.3	
28.6		14.2	
		23.7	

Appendix 11.7. the tongue tumor sections from syngeneic (a) and nude (b) mouses. Images are with 1.6x magnification. **a**. Tumor sections developed from mouse OSCC cells **b**. Tumor sections developed from human OSCC cells zenographts.

a

b